

# Beyond Safety Drivers: Staffing a Teleoperations System for Autonomous Vehicles

Andrew Daw

School of Operations Research and Information Engineering  
Cornell University  
257 Rhodes Hall, Ithaca, NY 14853  
amd399@cornell.edu

Robert C. Hampshire

Gerald R. Ford School of Public Policy  
University of Michigan Transportation Research Institute  
University of Michigan  
Weill Hall, Ann Arbor, MI 48109  
hamp@umich.edu

Jamol Pender

School of Operations Research and Information Engineering  
Cornell University  
228 Rhodes Hall, Ithaca, NY 14853  
jjp274@cornell.edu

November 8, 2021

## Abstract

Driverless vehicles promise a host of societal benefits including dramatically improved safety, increased accessibility, greater productivity, and higher quality of life. As this new technology approaches widespread deployment, both industry and government are making provisions for teleoperations systems in which remote human agents provide assistance to driverless vehicles. This assistance can involve real-time remote operation and even ahead-of-time input via human-in-the-loop artificial intelligence systems. In this paper, we address the problem of staffing such a remote support center. Our analysis focuses on the tradeoffs between the total number of remote agents, the reliability of the remote support system, and the resulting safety of the driverless vehicles. By establishing a novel connection between queueing models and storage processes, we determine the probability of the system exceeding its service capacity. This connection drives our staffing methodology. We also develop a numerical method

to compute the exact staffing level needed to achieve various performance measures. This moment generating function based technique may be of independent interest, and our overall staffing analysis may be of use in other applications that combine human expertise and automated systems.

## 1 Introduction

With automation poised to change a plethora of industries, the advent of autonomous vehicles stands out for the scope of its potential impacts. From major commercial freight to personal modes of transit, ground transportation will certainly be changed, and this means that there will be wide reaching effects throughout both commerce and culture; see Burns [8] for a comprehensive vision. As driverless car technology gets closer to public deployment, one of the most significant remaining problems is ensuring the safety of autonomous vehicles on public thoroughfares, both for their passengers and for those sharing the road with them. Currently, public testing of autonomous vehicles has required an **in-car safety driver**, but this is unrealistic for wide spread implementation so what else can be done to safeguard driverless cars? This question is of interest to both government and industry; legislation and LLCs alike are being created in response to it. For example, the state of California has recently introduced regulations requiring a **remote operator**, meaning a person not in the vehicle who can monitor and control the car when needed, for testing autonomous vehicles that are truly driverless and do not have a safety driver onboard, see California Department of Motor Vehicles [9]. Per Davies [13], this is also seen in the private sector, where both startups and major car companies are engineering new technology to ensure the safety, reliability, and efficiency of remote operator systems for autonomous vehicles. In this paper, we develop queueing models for this driverless car teleoperations system and determine the staffing levels that are needed to provide safe and reliable guidance to the autonomous vehicles.

In many ways, these teleoperations systems function much like a call center for driverless cars. When a vehicle encounters a situation it does not understand, it can **disengage** from its autonomous operation and call for help from a remote operator. A major driving force behind this idea is the realization that maintaining the safe operation of autonomous vehicles will require some type of human assistance, at least for the foreseeable future, see e.g. Koopman and Osyk [29]. While self-driving technology is both formidable and improving, the fact remains that there are too many edge cases; there are unknown unknowns. By introducing the opportunity to have human driver input in uncertain scenarios, these remote operator centers enable autonomous vehicles to function in environments they otherwise could not. Based on the mission statements of recent startups, this modern service system can cater to its driverless car customers in different ways. One type of service is the remote control of the vehicle. This involves a remote operator taking over the driving of the car for a period of time via a teleoperations system. An example of this technology used by the company Designated Driver is given in Figure 1.1. This is ideal for situations in which the operator can assume control in a relatively simple state and guide the car through an ambiguous environment ahead. For example, consider the pick up and drop off of passengers at a large airport terminal. Cars are often parked in strange locations and may start or stop unpredictably in pursuit of their own target gates. To a driverless vehicle this might

be overwhelmingly erratic behavior, but a remote human operator can easily steer the vehicle through the situation. We will refer to this kind of teleoperation service as **real-time remote operation**.



Figure 1.1: An example remote operation setup used by the startup Designated Driver [2].

For fast-paced, time critical situations, the remote operator center can employ a human-assisted AI based approach similar to what the startup Ottopia offers, as described in Sawers [42]. Through the recent work in Lundgard et al. [34], this type of service can even be accomplished in near real-time through an approach that uses human feedback on simulated states within reinforcement learning. In this method, driving input can be crowdsourced from a team of human agents. The idea of this technique for driverless car assistance is visualized in Figure 1.2. When the autonomous vehicle is approaching uncertainty ahead, it sends its current state information to the teleoperations center and requests support. Using this information, simulations of the cars future environment are generated and passed to a pool of remote operators. These operators then supply quick and specific driving instructions for each of the simulated scenarios, and this input is passed back to the vehicle before it encounters the time of the simulated scenarios. At that point in time, the autonomous vehicle can now reduce its uncertainty and determine an action via its library of human assistance, which spans a variety of possible environments. This approach can be viewed as a **human-in-the-loop system**, as the vehicle is operating through self-driving AI with occasional request for human input. Using language from Lundgard et al. [34], we refer to this human-assisted AI service as **look-ahead assistance** to distinguish it from the real-time remote operation service. By the nature of the simulation-based structure, this look-ahead method is well-equipped to provide quick instructions and feedback in time sensitive scenarios.

As one might expect, situations that demand fast responses are also often the most critical. Such can be seen in the first fatal accident involving a self-driving car, in which an Uber Technologies, Inc. autonomous vehicle hit and killed a pedestrian on the evening of March 18, 2018. During a test drive of a pre-determined route with an onboard operator, the Uber vehicle struck Elaine Herzberg as she was walking across

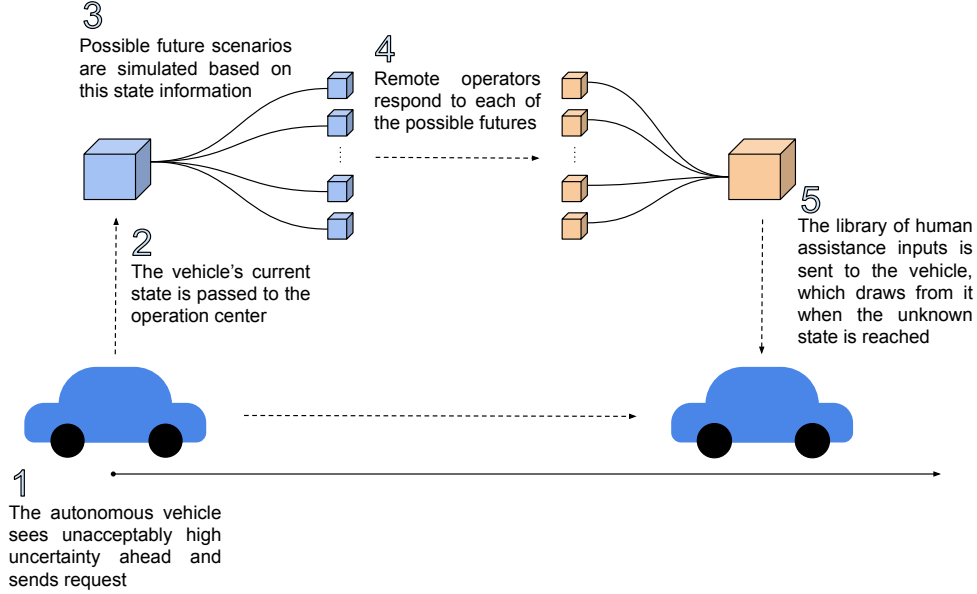


Figure 1.2: A visual guide to the human-assisted AI look-ahead service.

the lane of traffic with her bicycle. From the National Transportation Safety Board (NTSB) preliminary report of the incident [1], the self-driving system first identified an unknown object in the road approximately 6 seconds before the crash occurred. For the next 4.7 seconds the system struggled with uncertainty, classifying Ms. Herzberg as an unknown object, then as a vehicle, and then as a bicycle. Throughout these classifications, the software was additionally unsure of this unidentified figure’s future movement. It was not until 1.3 seconds before impact that the vehicle determined that emergency braking was needed. Tragically, the NTSB report states that according to Uber, emergency braking maneuvers were not enabled during testing for the sake of avoiding “erratic vehicle behavior” [1]. Furthermore, the system was not designed to alert the onboard operator and the operator did not notice the pedestrian until less than a second before the collision. A visualization of the location and paths from the NTSB report is shown in Figure 1.3.

We believe that the look-ahead approach could have served this situation in both direct and indirect ways. Directly, the human assistance based on the simulations of the environment could have significantly reduced the uncertainty the vehicle encountered. By both considering a wide variety of outcomes and receiving input from experienced human drivers, the car could have had been better equipped to make critical driving decisions. For an additional, indirect benefit, consider the vehicle’s underlying driving structure. As we have mentioned, the emergency braking had been disabled in order to “reduce the potential for erratic vehicle behavior,” per the NTSB report [1]. If this override is a reaction to the car being seen as overly cautious and braking too suddenly or frequently when it is unsure of how to proceed, then this too can be addressed by the look-ahead service. That is, when a vehicle encounters an uncertain situation and may apply emergency braking, it can receive verification on the decision to stop or not. Thus, no override would be needed and the emergency braking could be applied as intended. In this way, the look-ahead service allows the driverless car to function



Figure 1.3: Collision location and paths of the pedestrian and of the Uber test vehicle [1].

smoothly by receiving swift input from human experts when it needs it, including both instruction and assurance.

Combining the look-ahead assistance and real-time remote operation services, tele-operations systems can be designed to handle both rapid response and extended control scenarios. However, in order for these methods to be effective in helping autonomous vehicles operate safely, there must be sufficiently many remote agents available in the teleoperations support center. Because each type of service fundamentally depends on human input, it is critical that there is a large enough work force that the vehicles' requests for support can be answered promptly and accurately. Thus, this will be the guiding question of this work: how many remote operators are needed to staff a teleoperations center? While the answer certainly has financial implications for the car companies, startups, and government entities that have shown interest in autonomous vehicle teleoperations, this question is inherently about safety. Because the mission of these centers is to make driverless cars safe enough for public roads, finding the necessary number of workers is crucial.

To answer this question, we will model the teleoperations center as a queueing system. To capture a variety of settings and develop the tools of our analysis, we consider three different model types: an infinite server model, a finite server model with infinite buffer capacity (a delay model), and a finite server model with zero buffer capacity (a blocking model). In the look-ahead service context, we can note that this is a queueing model within a reinforcement learning problem or a Markov decision process, as described in [34]. Through the simulation of possible near-future states, the remote operators can be thought of as performing a just-in-time policy training when they provide input for the generated scenario. While we do not focus on this in depth in our analysis, the reinforcement learning context does serve as inspiration



to some of the assumptions for our model. Perhaps most importantly, this is one of the motivations that lead us to considering queueing models with batches of arrivals. The batch arrival of tasks to the teleoperations center will be a salient feature of our queueing models, particularly since we also show that batches capture bursts of arrivals. Through batches, we connect queueing models to storage processes. Because the storage processes literature is well-established, this connection allows us to leverage relevant results to answer this paper’s staffing questions. Finally, to support this analysis, we introduce a new numerical method for calculating a random variable’s cumulative distribution function through its moment generation function. Using this technique and the results from the storage processes literature, we can compute the probability of large-batch arrival queueing models exceeding their service capacities.

## 1.1 Review of Relevant Literature

Throughout the course of our analysis, we will see that bursts of arrivals have strong effects on the systems that they enter. This agrees with recent lines of work that study queueing models with bursty arrival processes, such as Gao and Zhu [19], Koops et al. [30, 31], Daw and Pender [14], L’Ecuyer et al. [33], Boxma et al. [5]. In these works, there are two main model characteristics that produce temporal clusters of arrival epochs: self-excitement and external stimuli. The classic examples of these processes are the Hawkes and Cox processes, respectively. Originally defined in Hawkes [26], the Hawkes process (in its simplest form) has an arrival intensity that jumps upward by a fixed amount when each arrival occurs and decays exponentially towards a baseline rate between epochs. Thus, this process is said to be self-exciting as the occurrence of an event increases the likelihood that another will occur soon after. Similarly, the analogous Cox process also has an arrival intensity with upward jumps and exponential decay, see e.g. Daley and Vere-Jones [11]. However, the times of these jumps are not the same as the arrival epochs; they are instead given by an external Poisson process. For this reason, the Cox process can be thought of a non-stationary Poisson process with stochastic intensity driven by another, exogenous Poisson process, and thus is often referred to as a doubly-stochastic Poisson process. We can note that self-excitement and external stimuli need not be mutually exclusive, as discussed briefly in Hawkes [26] and explored in depth in the “dynamic contagion process” introduced in Dassios and Zhao [12]. In this work, we show that both of these arrival bursts types can be represented as batch arrivals if the bursts are rapid enough.

One of the main ideas supporting our staffing analysis is the connection from batch arrival queueing systems to storage processes. We uncover the connections used in this work via a batch scaling in which the size of the batches grows large and the queue length process is scaled inversely. Similar albeit less general scalings have been explored recently in de Graaf et al. [17], Daw and Pender [16], although the limit was not characterized in Daw and Pender [16]. Specifically, the limits we prove in this work for the  $G^X/G/\infty$ ,  $G^X/M/cn$ , and  $G^X/M/cn/cn$  queues generalize the batch scaling results of  $M^X/M/\infty$  queueing systems shown in de Graaf et al. [17], Daw and Pender [16], which converge to shot noise processes with exponential decay. In this work, we extend beyond exponential decay and we also use a proof technique that does not impose a Poisson requirement on the arrival process. This allows us to make use of a broad literature on storage processes, which can be seen as a generalization of the shot noise processes. Storage processes, which can also be referred to as dams,

content processes, or even fluid queues, are positive valued, continuous time stochastic processes in which the process level will jump upwards by some amount at epochs given by a point process. Between jumps the process will decrease according to some function of its state. That is, there is a function, often denoted  $r : \mathbb{R}^+ \rightarrow \mathbb{R}^+$ , such that the rate of the process's decline when in state  $x$  is  $r(x)$ . For example,  $r(x) \propto x$  would recover the exponential decay of a shot noise process.

Because storage processes have a long history of study, we are able to draw upon a rich literature of interesting ideas. Many of the results that will be most relevant to us are focused on the stationary distributions of storage processes. Even on its own the study of stationary distributions of storage processes has a rich history, with early work including expressions of stationary distributions for shot noise processes given in Gilbert and Pollak [20]. Later work found similar results for more general settings, including Cinlar and Pinsky [10], Yeo [48, 47], Rubinovitch and Cohen [40], Kaspi [27]. A line of study that will be particularly useful for us can be found in Brockwell [7], Brockwell et al. [6], as these works find integral equations for the stationary distributions of storage processes with a general release rule  $r(\cdot)$ . These forms will be of great use to us in our staffing analysis. For precursors to this work in a different but no less interesting setting, see Harrison and Resnick [24, 25]. Another elegant area of study is the duality of the storage processes, for example see Kaspi and Perry [28], Perry and Stadje [36]. Connections between queues and storage processes are not new in general, as the single server queue has been known to be directly related to storage processes. For an overview of these connections and the related ideas, see Prabhu [37].

A key tool in our analysis will be the convergence of a sum of exponential functions to the indicator function  $\mathbf{1}\{x \leq c\}$ , as shown in Sullivan et al. [43]. This is of particular use to us in calculating the probability of a storage process exceeding a threshold, through which we drive our staffing analysis. One can note that an alternative approach to this would be to leverage asymptotic normality results, such as those in Lane [32], Rice [38] for shot noise processes. While this may work well in some settings, we can note that for systems that require a very rapid service rate, such as in the look-ahead service, the rate of arrivals may not be fast enough to justify a Gaussian approximation. This is of particular concern for approximating the tails of the distribution, which is at the heart of this problem.

## 1.2 Contributions and Organization

The remainder of this paper is organized as follows. In Section 2, we model the autonomous vehicle teleoperations center as a queueing system with batch arrivals. We take care to motivate the batches and show that batches capture the rapid bursts of arrivals that can occur in this setting. In particular, Proposition 2.1 relates batches to sudden external stimuli and Proposition 2.2 shows that batches arise out of sudden self-excitement. We then connect these queueing models to storage processes through three batch scaling results. Specifically, Theorem 2.3 shows that infinite server models converge to shot noise processes, Theorem 2.4 shows that delay models converge to storage processes with threshold release rule, and Theorem 2.5 shows that blocking models converge to finite capacity storage processes. In Section 3, we use these storage processes to obtain staffing levels for the teleoperations center. By use of Lemma 3.3, which computes quantities such as the cumulative distribution function through sums based on the moment generating function and Legendre polynomial coefficients, we

find asymptotic expressions for the probability of these delay and blocking processes exceeding capacity in Theorems 3.4 and 3.5, respectively. We demonstrate the performance of our results and numerical techniques in Section 4. We note that although the scope and interest of this paper is in staffing a teleoperations system for driverless vehicles, the techniques we develop for this analysis may be of use in many other problems in applied probability. Furthermore, the concepts of this paper may also extend to applications beyond autonomous vehicles, as the idea of human support for automated processes may be of use in many different areas.

## 2 Modeling the Remote Support Center Using Queueing Theory

In the introduction, we discussed two types of service that could be offered in an autonomous vehicle teleoperations system: look-ahead assistance and real-time remote operation. As we will describe throughout this section, both of these can be modeled as queueing systems. In each setting, autonomous vehicles send requests for support to the teleoperations center. These requests are then handled by the remote agents. If the support type is look-ahead assistance the agents' responses are then sent back to the vehicle, and if the support type is real-time remote operation the agent will assume live remote control of the vehicle until the situation is resolved. In this section, we use these service dynamics as motivation in building queueing models that feature batch arrivals. Specifically, we will consider three different queueing systems: an infinite server queue, a multi-server queue with infinite buffer (i.e. a delay model), and a multi-server queue with no buffer (i.e. a blocking model). We will denote these models  $Q_t(n)$ ,  $Q_t^C(n)$ , and  $Q_t^B(n)$ , respectively. We motivate, define, and analyze these models in this section. In Subsection 2.1, we explore the variety of reasons that batches should be used in modeling this teleoperations center. In Subsection 2.2, we then use these ideas to formally define the queueing models and, in Subsection 2.3, we use the batch structure to uncover a connection between these queueing models and storage processes.

### 2.1 Bursts of Requests, Batches of Arrivals

A key notion in this paper is that requests for support will arrive in bursts, or temporally clustered flurries of occurrences. We will model these bursts as batches, meaning a potentially random number of requests that occur simultaneously. In this subsection, we motivate both the reasons why bursts of requests will occur and the reasons why we can treat these bursts as batches of concurrent arrivals. To begin, we address why requests occur in bursts, which can be distilled to three main reasons.

First, there are wide-spread exogenous factors that can affect many vehicles in rapid fashion. As an example of this, consider sudden inclement weather. If a strong storm forms unexpectedly, a large number of vehicles may encounter heightened uncertainty and send requests to disengage from their standard driverless car operation and receive human help, either in the form of brief assistance via the look-ahead approach or in extended support by way of real-time remote operation. In fact, this type of bursts has already occurred in practice, as documented by the 2018 California disengagement reports. On Nov. 11<sup>th</sup>, 2018, Waymo reported that multiple vehicles disengaged from



autonomous operation due to “adverse weather conditions experienced during testing” [45]. As the number of driverless vehicles on the road grows, these external shocks have the potential to affect more vehicles more often.

As a second factor leading to bursts, we can observe the contagious nature of the very disengagements themselves. This phenomenon stems from the fact that disengagements occur when an autonomous vehicle can’t reliably predict or interpret its environment, i.e. when a car encounters intolerably high uncertainty. By receiving either remote assistance or remote operation, the driverless car then goes “off algorithm.” The vehicle is thus inherently acting in a way that it could not confidently predict for itself; otherwise, it would not need to disengage. For this reason, the disengagement itself can be a hazard to other nearby autonomous vehicles. Any other driverless vehicles in this car’s vicinity are then subjected to added uncertainty, as they likely cannot confidently predict the behavior of the disengaged car either. This then leads to a higher risk of these neighboring vehicles disengaging, which can then spread to other vehicles in their own vicinity, and so on. This epidemic behavior has been shown to induce self-exciting arrival patterns, e.g. in Rizoiu et al. [39], Daw and Pender [15]. This too can be seen in the California disengagement reports, as industry leaders such as Waymo and GM Cruise list other vehicles behaving “poorly” or “recklessly” and “incorrect behavior prediction” of other road users as common reasons for disengaging the autonomous operation of their vehicles, see GM Cruise LLC [21], Waymo LLC [45].

Third, we can also recognize that there is an inherent self-exciting nature to exploration in reinforcement learning, particularly so in undirected exploration scenarios. We will assume that this must be the type of exploration that applies to publicly deployed autonomous vehicles, as directing customer travel into uncertainty is likely too much of a liability simply for the sake of exploration. As an illustrative example based on Thrun [44], consider a random walk as a proxy for undirected exploration over a vast state space. When the process encounters a new state it is at the periphery of its understanding and is thus likely connected to other unknown, unvisited states. Therefore, the process is more likely to encounter another new state than it is when it is in the interior of its process history. Thus, encountering an unknown state increases the likelihood of entering another unknown state soon afterwards, which matches the idea of self-excitement. Since there are unknown unknowns in the reinforcement learning model for autonomous vehicles, new states can be encountered indefinitely.

We now demonstrate that batches can capture the phenomena of bursts of arrivals. We have identified two types of bursts, external stimuli and self-excitement, and we will examine each individually. First, we consider an arrival process with intensity subject to exogenous shocks. That is, suppose that for a duration that is exponentially distributed with rate  $\beta_E > 0$  arrivals occur with exponentially distributed intervals at rate  $\alpha_E > 0$ . Note that this is an ephemeral, external shock to the process arrival rate, as it increases by a fixed amount for a random duration. This creates a cluster of arrivals. We define this arrival cluster through two quantities: the cluster duration  $\tau_E$  and the cluster size  $\chi_E$ . That is, let  $\tau_E$  be the length of time from when the shock first increases the arrival rate to when the shock ends. Additionally, let  $\chi_E$  be the number of arrivals that occur during this time as a result of the increased arrival rate. Then, in Proposition 2.1 we see that as the external shock becomes increasingly sudden, this cluster becomes a batch.

**Proposition 2.1.** *As  $\alpha_E$  and  $\beta_E$  simultaneously grow large with  $p \equiv \frac{\beta_E}{\alpha_E + \beta_E}$  fixed,*

the expected duration of a shock becomes arbitrarily small, i.e.  $\frac{1}{\beta_E} \rightarrow 0$ , while the size of the arrival cluster remains geometrically distributed with success probability  $p$ , thus yielding a batch.

*Proof.* Let us formalize this simultaneous scaling by re-defining the intensity increase and expiration rate as  $\alpha_E x$  and  $\beta_E x$ , respectively. Then, by definition  $\tau_E \sim \text{Exp}(\beta_E x)$  and thus

$$\mathbb{E}[\tau_E] = \frac{1}{\beta_E x} \rightarrow 0,$$

as  $x \rightarrow \infty$ . Then, the number of arrivals during this time has distribution  $\chi_E \sim \text{Pois}(\alpha_E \tau_E x)$ , which is known to be geometrically distributed. This geometric can be observed through manipulation of the moment generating function using the tower property and simplifying:

$$\mathbb{E}[e^{\theta \chi_E}] = \mathbb{E}\left[\mathbb{E}[e^{\theta \chi_E} \mid \tau_E]\right] = \mathbb{E}\left[e^{\alpha_E \tau_E x (e^\theta - 1)}\right] = \frac{\beta_E x}{\beta_E x - \alpha_E x (e^\theta - 1)} = \frac{p e^\theta}{1 - (1 - p) e^\theta}.$$

Because this does not depend on  $x$ , we have completed the proof.  $\square$

As a consequence of Proposition 2.1, we observe that if the duration of a burst from external stimuli is much shorter than the overall arrival rate or the staffing window, then this sort of shock can be modeled as a batch.

We can draw a similar conclusion for clusters of arrivals driven by self-excited contagion. To observe this, consider an arrival process that is ephemerally self-exciting, as described in Daw and Pender [15]. That is, at the occurrence of each arrival, the process intensity increases by an amount  $\alpha_S > 0$  for a duration that is independently and exponentially distributed with rate  $\beta_S > \alpha_S$ . In this way, each arrival raises the rate of future arrivals and, by consequence, increases the likelihood of another arrival occurring soon afterwards. However, this only takes place for a finite amount of time, after which the arrival's effect on the process intensity vanishes. This creates a temporal cluster of arrivals, which we again define through a cluster duration  $\tau_S$  and a cluster size  $\chi_S$ . We let  $\tau_S$  be the time from when the first arrival occurs to the departure of the last entity caused by this initial arrival or by the descendants of it. Similarly, we let  $\chi_S$  be the total number of arrivals caused by this arrival and its descendants, including the initial arrival itself.

Because the inter-arrival and inter-departure times are all exponentially distributed, we can also define  $\tau_S$  and  $\chi_S$  in terms of a continuous time Markov chain, specifically a linear birth-death process which we denote will denote  $X_t$ . That is, let the Markov chain  $X_t$  have state space given by the natural numbers  $\mathbb{N}$ . When the process is in state  $k$  let the arrival rate be  $\alpha_S k$  and let the departure rate be  $\beta_S k$ . We can then note that state 0 is an absorbing state. Suppose that the initial arrival occurred at time 0 and let the chain start in state 1. Then, we can define  $\tau_S$  as the time until the chain is absorbed into state 0 and  $\chi_S$  as the number of up-jumps before the chain is absorbed into state 0, plus one for the initial arrival. Then, in Proposition 2.2 we find that as this contagion becomes increasingly rapid this self-excited arrival cluster becomes a batch.

**Proposition 2.2.** *As  $\alpha_S$  and  $\beta_S$  grow large simultaneously with  $\eta \equiv \frac{\alpha_S}{\beta_S}$  fixed, the expected time duration of a self-excited arrival cluster becomes arbitrarily small, i.e.*

$$\mathbb{E}[\tau_S] \rightarrow 0 \text{ as } \alpha_S, \beta_S \rightarrow \infty, \quad (2.1)$$

whereas the distribution of the arrival cluster size remains unchanged, with probability mass function given by

$$P(\chi_S = k) = \frac{1}{k} \binom{2k-2}{k-1} \left( \frac{1}{\eta+1} \right)^k \left( \frac{\eta}{\eta+1} \right)^{k-1}, \quad (2.2)$$

for all  $k \in \mathbb{Z}^+$ , thus yielding a batch.

*Proof.* As in Proposition 2.1, let us re-define the intensity jump size and the duration rate as  $\alpha_S x$  and  $\beta_S x$ , respectively, where  $x > 0$ . By use of Proposition 4.5 of Daw and Pender [15], we can note that the expected time duration of the cluster is such that

$$E[\tau] = \frac{1}{\alpha_S x} \log \left( \frac{\beta_S x}{\beta_S x - \alpha_S x} \right) = \frac{1}{\alpha_S x} \log \left( \frac{\beta_S}{\beta_S - \alpha_S} \right) \rightarrow 0,$$

as  $x \rightarrow \infty$ . Then, from Proposition 4.3 in Daw and Pender [15], we can further note that the probability mass function of the size of the cluster is given by

$$\begin{aligned} P(\chi_S = k) &= \frac{1}{k} \binom{2k-2}{k-1} \left( \frac{\beta_S x}{\beta_S x + \alpha_S x} \right)^k \left( \frac{\alpha_S x}{\beta_S x + \alpha_S x} \right)^{k-1} \\ &= \frac{1}{k} \binom{2k-2}{k-1} \left( \frac{\beta_S}{\beta_S + \alpha_S} \right)^k \left( \frac{\alpha_S}{\beta_S + \alpha_S} \right)^{k-1}, \end{aligned}$$

and this does not depend on  $x$ . By normalizing each fraction by  $\beta_S$ , we simplify to the stated form with  $\eta$ .  $\square$

Just as we observed in Proposition 2.1, this now implies that if the rate of contagion in a self-excited cluster is much faster than the overall arrival rate or the staffing time scale then the self-excited cluster can be modeled as a batch.

As a final motivation for batch arrivals, we turn to a fundamental component of this problem. That is, the very structure of the look ahead assistance involves a batch, as can be seen in Figure 1.2. Because these jobs are multiple simulated situations based on the current conditions of the car, these are inherently batches of arrivals occurring at the remote support center. For each individual disengagement there are many tasks sent to the system. Hence, the human-in-the-loop assistance creates batches of tasks at each arrival of support requests. Furthermore, these batch sizes may be quite large because many simulated future states may need to be examined, as the state space is complex and vast. In fact, in practice the teleoperations system may use intentional redundancy for the sake of safety and send duplicates of each task to crowdsource responses, as is described in Lundgard et al. [34]. Additionally, because of the multiple causes of batches and bursts in this system, the resulting arrival structure may actually be batches of batches of jobs. Thus, in this work we study the system for large batch sizes and seek to understand the process performance as the batch size scales.

## 2.2 Defining the Queueing Models with Batch Arrivals

Recall that in our study of autonomous vehicle teleoperations centers, we are studying three different queueing models: an infinite server model  $Q_t(n)$ , a delay model  $Q_t^C(n)$ , and a blocking model  $Q_t^B(n)$ . Let us now formally define these queueing systems. In all

three models, batches of entities enter the system simultaneously at each arrival epoch. Each arrival epoch corresponds to a request for support from a vehicle, the arriving entities each represent a support task from an autonomous vehicle, and each server is a remote operator. Because the differences between look-ahead assistance and real-time operation are primarily in the speed of service or in the structure of the batch arrivals, we will not distinguish between the two settings when developing analytic results in this section or in Section 3. The approach we take will be general and thus can apply to both service regimes. We explore the staffing differences implied by the two relative parameter sizes numerically in Section 4. We formally define the individual details of each model as follows, starting with the infinite server system.

Let  $Q_t(n)$  be the number in system for an infinite server queue at time  $t \geq 0$ , where  $n \in \mathbb{Z}^+$  relates to the size of the arrival batches. Suppose that arrivals occur in batches at epochs given by a point process  $N_t$ . Let the  $i^{\text{th}}$  batch size be drawn from the sequence of independent, positive, integer random variables  $\{B_i(n) \mid i \in \mathbb{Z}^+, n \in \mathbb{Z}^+\}$ , where  $B_i(n)$  are identically distributed across all  $i$  for fixed  $n$ , with  $\mathbb{E}[B_1(n)] \in O(n)$ , meaning that the average batch size grows linearly with  $n$ . We suppose that each entity within the batch receives individual service that starts immediately upon the occurrence of their arrival. Let the service duration in the queue be independent and identically distributed with cumulative distribution function  $G(\cdot)$ . In Kendall notation, this is the  $G^{B_1(n)}/G/\infty$  queueing system.

Next, let  $Q_t^C(n)$  be the queue length process for a  $G^{B_1(n)}/M/cn$  queue, the delay model. That is, let  $Q_t^C(n)$  be the number of entities in system at time  $t \geq 0$  for a queue that receives arrivals in batches with size drawn from the sequence  $\{B_i(n) \mid i \in \mathbb{Z}^+, n \in \mathbb{Z}^+\}$  at epochs given by the point process  $N_t$ , as defined for the infinite server system  $Q_t(n)$ . By comparison to that model, suppose that this queueing system has  $cn$  servers where  $c > 0$  and that the service lengths are independent and exponentially distributed with rate  $\mu > 0$ . Furthermore,  $cn$  is assumed to be an integer. When each batch arrives, each available server will begin serving one of the arriving entities. If there are not enough idle servers, the remaining entities in the batch will wait one-by-one for ongoing service to be completed. We can note that an equivalent Kendall notation for this model is  $G^{B_1(n)}/M/cn/\infty$ , as there is space for infinitely many entities to wait. Note that in this construction  $c$  is not a number of servers but rather a ratio between the number of servers and the relative batch size  $n$ .

Finally, for the blocking model we let  $Q_t^B(n)$  be the queue length process for a  $G^{B_1(n)}/M/cn/cn$  queue. That is, let  $Q_t^B(n)$  be the number of entities in system at time  $t \geq 0$  for a queue that receives arrivals in batches with size drawn from the sequence  $\{B_i(n) \mid i \in \mathbb{Z}^+, n \in \mathbb{Z}^+\}$  at times given by the point process  $N_t$ . Furthermore, suppose that this queueing system has both  $cn$  servers and  $cn$  capacity, where  $c > 0$  and  $cn$  is assumed to be an integer, and that the service lengths are independent and exponentially distributed with rate  $\mu > 0$ . Suppose that the queue features partial blocking of batches, i.e. any batch of arrivals that exceeds the number of available servers will admit only as many entities as there are servers available. Thus, no entities wait for service but not all arriving entities are served. Again we note that in this case  $c$  is the ratio between the number of servers and the relative batch size  $n$ .

Each of these models gives us a different perspective on how the system could possibly operate. For example, the infinite server model represents the ideal scenario. Every request is immediately answered and no tasks wait. While it is of course unrealistic to

have an infinitely large work force, the  $Q_t(n)$  model gives us an idea of the best case performance of the teleoperations system. Furthermore, the relative tractability of the infinite server model can often be of use in analyzing the other two scenarios, as we will see. While they may be more difficult to analyze than the infinite server queue, the delay model  $Q_t^C(n)$  and the blocking model  $Q_t^B(n)$  give us more realistic perspectives under two different philosophies. For the delay model, arriving requests that find all remote operators busy will wait until an agent becomes available whereas in the blocking model any task that finds no operators available will never be served, i.e. it is “blocked.” While the delay model is a realistic representation of many scenarios, we can note that the blocking model stresses a particular urgency that can be relevant in the look-ahead crowdsourcing regime. In this case, responses may be needed within a very short time window and so any waiting at all may not be feasible. This also falls under the general goal in both the blocking and the delay model, which is to find a staffing level for the teleoperations center so that the probability of a request not being immediately answered achieves a specified target level.

In considering these three different systems as a whole, their salient, uniting feature is batch arrivals. As discussed in Subsection 2.1, these batches capture the bursts of arrivals that can occur from external stimuli, self-excited contagion, the forward simulations, and even from the process of exploration itself. In the following subsection, we use this batch structure to find connections to shot noise processes, dams, and storage processes.

## 2.3 From Queues to Storage Processes

To motivate the concept of what we will refer to as a “batch scaling” of a queueing system, let us make an informal comparison to a queue’s fluid limit. Like in a fluid limit, imagine shrinking the size of each arriving entity in a queueing model. However, rather than increasing the rate that entities arrive, like in the fluid limit, suppose that instead we increase the number of entities that enter the system at each arrival epoch. In this way, we isolate the arrival process; the distribution of the inter-arrival times is the same for all  $n$  whereas the distribution queue’s departure process changes with  $n$ . In the limit, we find that these batch scaled queueing processes converge to storage processes, which have also been referred to as dams or even fluid queues. Informally, the idea of these continuous time processes is as follows. Much like how in this work we think of a queue by its queue length, i.e. the number of entities present in the system at the given time, a storage process is concerned with the total “content” currently in system. By comparison to the queue this content is a non-negative real number, rather than a non-negative integer. Like a queue, the content in the storage process jumps upward by some amount at times given by some point process, but unlike the queue, the content in the storage process simply drains or releases deterministically between the jump epochs. We will refer to the manner in which the content drains as the “release rule” of the storage process, which may depend on the current content level. In this way one can see how these processes have been a natural fit in the literature for modeling dams, as the jumps can represent an amount of water added to the reservoir in sudden, large amounts such as from rainfall, whereas the release from draining or evaporation is gradual and continuous. While this informal discussion of the model is intended to guide intuition for the process, we will formally define the various storage processes in this work upon their introduction.



As a preliminary, we now introduce the notation and assumptions that we will use throughout our batch scaling analysis. At the risk of overloading notation, we will let  $N_t$  be a point process that is equivalent in distribution to the process for the queue arrival epochs (thus we do not use distinguishing notation) and we let  $A_i$  be the corresponding  $i^{\text{th}}$  arrival epoch. Furthermore, we let  $\bar{G}(x) = 1 - G(x)$  for all  $x \geq 0$  where  $G(\cdot)$  is the cumulative distribution function for the service in the queueing model. Then, we suppose that there is an i.i.d. sequence of positive random variables  $\{M_i \mid i \in \mathbb{Z}^+\}$  such that  $\frac{B_1(n)}{n} \xrightarrow{D} M_1$  as  $n \rightarrow \infty$ , with  $\frac{B_1(n)}{n^2} \xrightarrow{p} 0$ . In this assumption, the batch scaling of the queue converts discrete batches of entities to continuous jumps in content, or “marks.”

Using these terms and assumptions, we will now prove three different batch scaling results, one for each of the three different queueing models,  $Q_t(n)$ ,  $Q_t^C(n)$ , and  $Q_t^B(n)$ . Beginning with  $Q_t(n)$ , we will now show the convergence of  $G^{B_1(n)}/G/\infty$  queues to general shot noise processes, which can be viewed as infinite capacity storage, or dam, processes. That is, let the shot noise process  $\psi_t$  at time  $t \geq 0$  be defined as

$$\psi_t = \sum_{i=1}^{N_t} M_i \bar{G}(t - A_i), \quad (2.3)$$

which will have jumps upward according to the sequence  $\{M_i \mid i \in \mathbb{Z}^+\}$  and then decay downward according to the kernel given by the complementary CDF  $G(\cdot)$ . This can be thought of as an infinite capacity storage process, as there is no bound on the amount of content that can enter the system at once. Furthermore, as in an infinite server queue, the manner in which the content brought by one arrival departs has no dependance on any of the arrivals before it or on the amount of the content currently in the system. Following this intuition, we now formalize the connections between the shot noise process and the general infinite server queue in Theorem 2.3.

**Theorem 2.3.** *As  $n \rightarrow \infty$ , the batch scaling of the  $G^X/G/\infty$  queue  $Q_t(n)$  yields*

$$\frac{Q_t(n)}{n} \xrightarrow{D} \psi_t, \quad (2.4)$$

pointwise in  $t \geq 0$ , where  $\psi_t$  is a shot noise process as defined in Equation 2.3, i.e. an infinite capacity storage process. If  $N_t$  is a Poisson process, this implies that the moment generating function of  $\frac{Q_t(n)}{n}$  converges to

$$\mathbb{E} \left[ e^{\frac{\theta}{n} Q_t(n)} \right] \longrightarrow e^{\lambda \int_0^t (\mathbb{E}[e^{\theta M_1 \bar{G}(x)}] - 1) dx}, \quad (2.5)$$

as  $n \rightarrow \infty$ .

*Proof.* We will show the convergence of the batch scaling of the queue through analyzing its moment generating function. To begin, we note that the infinite server queue length can be expressed in terms of indicator functions as

$$Q_t(n) = \sum_{i=1}^{N_t} \sum_{j=1}^{B_i(n)} \mathbf{1}\{t < A_i + S_{i,j}\},$$

where  $S_{i,j}$  is the service duration of the  $j^{\text{th}}$  customer within the  $i^{\text{th}}$  batch, and thus we can write the moment generating function of  $Q_t(n)$  at  $\frac{\theta}{n}$  as

$$\mathbb{E} \left[ e^{\frac{\theta Q_t(n)}{n}} \right] = \mathbb{E} \left[ \exp \left( \frac{\theta}{n} \sum_{i=1}^{N_t} \sum_{j=1}^{B_i(n)} \mathbf{1}\{t < A_i + S_{i,j}\} \right) \right].$$

By conditioning on the filtration of the counting process  $\mathcal{F}_t^N$ , total expectation yields that

$$\mathbb{E} \left[ \exp \left( \frac{\theta}{n} \sum_{i=1}^{N_t} \sum_{j=1}^{B_i(n)} \mathbf{1}\{t < A_i + S_{i,j}\} \right) \right] = \mathbb{E} \left[ \prod_{i=1}^{N_t} \mathbb{E} \left[ \exp \left( \frac{\theta}{n} \sum_{j=1}^{B_i(n)} \mathbf{1}\{t < A_i + S_{i,j}\} \right) \middle| \mathcal{F}_t^N \right] \right].$$

Focusing on the inner expectation, we again use the tower property. We now condition on the batch size  $B_i(n)$ , which leaves the service duration as the only uncertain quantity. The indicator is thus a Bernoulli random variable with success probability  $\bar{G}(t - A_i)$ , and since these are i.i.d. within the batch we have that

$$\begin{aligned} \mathbb{E} \left[ \exp \left( \frac{\theta}{n} \sum_{j=1}^{B_i(n)} \mathbf{1}\{t < A_i + S_{i,j}\} \right) \middle| \mathcal{F}_t^N \right] &= \mathbb{E} \left[ \prod_{j=1}^{B_i(n)} \mathbb{E} \left[ e^{\frac{\theta}{n} \mathbf{1}\{t < A_i + S_{i,j}\}} \middle| \mathcal{F}_t^N, B_i(n) \right] \middle| \mathcal{F}_t^N \right] \\ &= \mathbb{E} \left[ \left( G(t - A_i) + \bar{G}(t - A_i) e^{\frac{\theta}{n}} \right)^{B_i(n)} \middle| \mathcal{F}_t^N \right] \\ &= \mathbb{E} \left[ \left( 1 + \bar{G}(t - A_i) (e^{\frac{\theta}{n}} - 1) \right)^{B_i(n)} \middle| \mathcal{F}_t^N \right]. \end{aligned}$$

By now using the identity  $x = e^{\log(x)}$ , we can transform this to

$$\begin{aligned} \mathbb{E} \left[ \left( 1 + \bar{G}(t - A_i) (e^{\frac{\theta}{n}} - 1) \right)^{B_i(n)} \middle| \mathcal{F}_t^N \right] &= \mathbb{E} \left[ \exp \left( \log \left( \left( 1 + \bar{G}(t - A_i) (e^{\frac{\theta}{n}} - 1) \right)^{B_i(n)} \right) \right) \middle| \mathcal{F}_t^N \right] \\ &= \mathbb{E} \left[ e^{B_i(n) \log \left( 1 + \bar{G}(t - A_i) (e^{\frac{\theta}{n}} - 1) \right)} \middle| \mathcal{F}_t^N \right], \end{aligned}$$

which we can now re-express further through two series expansions. Specifically, using a Taylor and a Mercator series expansion on  $e^{\frac{\theta}{n}} - 1$  and  $\log \left( 1 + \bar{G}(t - A_i) (e^{\frac{\theta}{n}} - 1) \right)$ , respectively, we simplify to

$$\mathbb{E} \left[ e^{B_i(n) \log \left( 1 + \bar{G}(t - A_i) (e^{\frac{\theta}{n}} - 1) \right)} \middle| \mathcal{F}_t^N \right] = \mathbb{E} \left[ e^{\frac{\theta B_i(n) \bar{G}(t - A_i)}{n} + O\left(\frac{B_i(n)}{n^2}\right)} \middle| \mathcal{F}_t^N \right].$$

Returning to the original expectation, we now have that

$$\mathbb{E} \left[ \prod_{i=1}^{N_t} \mathbb{E} \left[ \exp \left( \frac{\theta}{n} \sum_{j=1}^{B_i(n)} \mathbf{1}\{t < A_i + S_{i,j}\} \right) \middle| \mathcal{F}_t^N \right] \right] = \mathbb{E} \left[ e^{\sum_{i=1}^{N_t} \frac{\theta B_i(n) \bar{G}(t - A_i)}{n} + O\left(\frac{B_i(n)}{n^2}\right)} \right],$$

and as  $n \rightarrow \infty$ , this converges to

$$\mathbb{E} \left[ e^{\sum_{i=1}^{N_t} \frac{\theta B_i(n) \bar{G}(t - A_i)}{n} + O\left(\frac{B_i(n)}{n^2}\right)} \right] \longrightarrow \mathbb{E} \left[ e^{\theta \sum_{i=1}^{N_t} M_i \bar{G}(t - A_i)} \right],$$

which yields the stated result for the queue. To now yield the specific form of the generating function when  $N_t$  is a Poisson process, we note that when conditioned on the quantity  $N_t$  we have

$$\mathbb{E} \left[ e^{\sum_{i=1}^{N_t} \theta M_i \bar{G}(t-A_i)} \right] = \mathbb{E} \left[ \mathbb{E} \left[ e^{\sum_{i=1}^{N_t} \theta M_i \bar{G}(t-A_i)} \mid N_t \right] \right] = \mathbb{E} \left[ \mathbb{E} \left[ e^{\theta M_1 \bar{G}(U_1(0,t))} \right]^{N_t} \right],$$

where  $U_i(0,t) \sim \text{Uni}(0,t)$  are i.i.d and independent of  $M_i$ . Then, conditioning on  $M_1$ , this inner expectation can be expressed

$$\mathbb{E} \left[ e^{\theta M_1 \bar{G}(U_1(0,t))} \right] = \mathbb{E} \left[ \mathbb{E} \left[ e^{\theta M_1 \bar{G}(U_1(0,t))} \mid M_1 \right] \right] = \mathbb{E} \left[ \frac{1}{t} \int_0^t e^{\theta M_1 \bar{G}(x)} dx \right].$$

By exchanging the order of integration and expectation via Fubini's theorem and substituting into the moment generating function for the Poisson process, we achieve the corresponding stated form.  $\square$

For a visual example of this convergence, in Figure 2.1 we plot the empirical distributions of four infinite server queues with different batch sizes and compare them to the simulated distribution of the limiting shot noise process. In this scenario the batches are Poisson distributed with rate  $n$  and through the scaling this produces deterministic jumps of size 1 in the storage process. As one can observe, as the batch size increase the queue's cumulative distribution function becomes increasingly similar to the cumulative distribution function for the shot noise process.

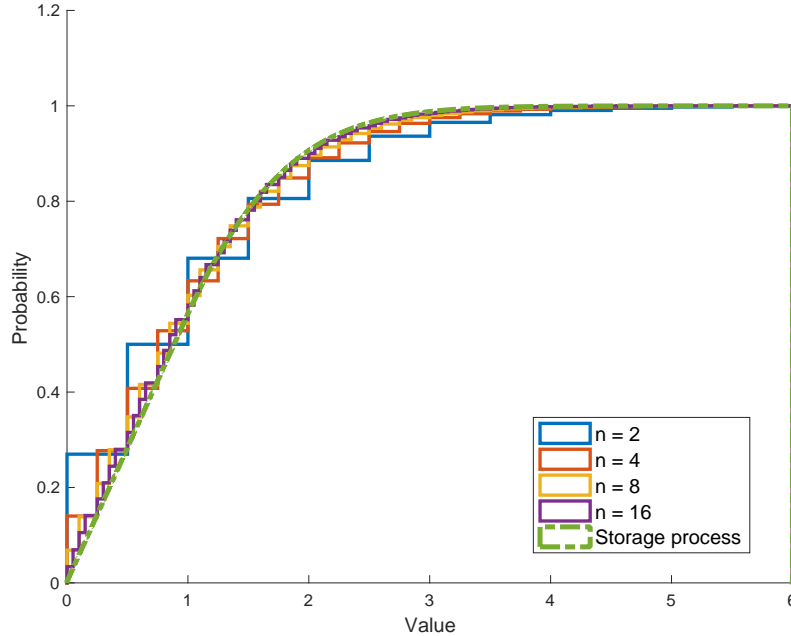


Figure 2.1: Simulated demonstration of convergence in distribution of an  $M^X/M/\infty$  queue to a shot noise process, based on 100,000 replications with  $t = 10$ ,  $\lambda = 1$ ,  $\mu = 1$ , and  $B_1(n) \sim \text{Pois}(n)$ .

If we specify the infinite server queue's service distribution as exponential with rate  $\mu > 0$ , we can note that the time until the next departure is exponentially distributed with rate  $\mu k$  if the current queue length is  $Q_t(n) = k$ . We can observe an analogous behavior in the shot noise process: if  $\bar{G}(s) = e^{-\mu s}$ , then the rate of release for  $\psi_t = x$  will be  $\mu x$ . With this in mind, we find a similar structure for the  $G^{B_1(n)}/M/cn$  delay model  $Q_t^C(n)$ . For the sake of example, let us consider the case  $n = 1$ . If the queue length is  $Q_t^C(1) = k$ , the time until the next departure is exponentially distributed with rate equal to either  $\mu k$  or  $\mu c$ , depending on which is smaller. Specifically, we can describe the departure rate as  $\mu(c \wedge k)$  when  $Q_t^C(1) = k$  and for  $n \geq 2$  we can generalize this to  $\mu(cn \wedge k)$  for  $Q_t^C(n) = k$ . Following the intuition provided by the infinite server case, we define the process  $\psi_t^C$  for time  $t \geq 0$  such that

$$\psi_t^C = \psi_0^C + J_t - \mu \int_0^t (\psi_s^C \wedge c) ds, \quad (2.6)$$

which we will refer to as the storage process with  $c$ -threshold rule, as we can define the release rate as  $r(x) \equiv \mu(x \wedge c)$  when  $\psi_t^C = x$ . Just as the  $G^{B_1(n)}/M/cn$  queue can serve no faster than its  $cn$  servers can collectively work, the  $c$ -threshold storage process can drain no faster than  $c$  times the base release rate  $\mu$ . With the assumption that the initial values of the queue and the storage process are known and converge to one another  $\frac{Q_0^C(n)}{n} \rightarrow \psi_0^C$ , we show convergence in distribution of the delay queueing model to a storage process with threshold release rule now in Theorem 2.4.

**Theorem 2.4.** *As  $n \rightarrow \infty$ , the batch scaling of the  $G^X/M/cn$  queue  $Q_t^C(n)$  yields*

$$\frac{Q_t^C(n)}{n} \xrightarrow{D} \psi_t^C, \quad (2.7)$$

pointwise in  $t \geq 0$ , where  $\psi_t^C$  is a storage process with  $c$ -threshold release rule as defined in Equation 2.6.

*Proof.* Because the distribution of the arrival epochs is unchanged as the batch size grows, we can note that by definition these times are equivalent to the jump times of the storage process. We start with the behavior up to the first arrival. Assuming  $0 \leq t < A_1$ , we can note that the queue length  $Q_t^C(n)$  is equal in distribution to

$$Q_t^C(n) \stackrel{D}{=} (Q_0^C(n) - cn - Z_t(n) \vee 0) + \sum_{i=1}^{cn \wedge Q_0^C(n)} \mathbf{1}\{S_i + \tau_n > t\},$$

where  $\{S_i \mid i \in \mathbb{Z}^+\}$  is an i.i.d. sequence equal in distribution to the service duration,  $Z_t(n)$  is a Poisson process with rate  $cn\mu$  that is independent from the  $S_i$  sequence, and  $\tau_n$  is a stopping time defined  $\tau_n = \inf_{t \geq 0} \{Z_t(n) = Q_0^C(n) - cn\}$ . Recall that no arrivals happen on this interval by definition. For intuition, one can view the first term on the right hand side as handling all the departures from the queue while the system is above capacity. Likewise, the summation handles the departures that occur once the queue length is less than or equal to the number of servers, which happens at time  $\tau_n$ . Now, dividing this expression by  $n$ , we have

$$\frac{Q_t^C(n)}{n} \stackrel{D}{=} \left( \frac{Q_0^C(n)}{n} - c - \frac{Z_t(n)}{n} \vee 0 \right) + \frac{1}{n} \sum_{i=1}^{cn \wedge Q_0^C(n)} \mathbf{1}\{S_i + \tau_n > t\},$$

we can now reason about its limiting behavior as  $n \rightarrow \infty$ . The elementary renewal theorem for Poisson processes gives that  $\frac{Z_t(n)}{n} \xrightarrow{a.s.} c\mu t$  as  $n \rightarrow \infty$ , and thus by the continuous mapping theorem

$$\left( \frac{Q_0^C(n)}{n} - c - \frac{Z_t(n)}{n} \vee 0 \right) \xrightarrow{a.s.} (\psi_0^C - c - c\mu t \vee 0),$$

where we have used the assumption for the convergence of the initial values. Thus, we can observe that the stopping time  $\tau_n$  is such that

$$\tau_n = \inf_{t \geq 0} \left\{ \frac{Z_t(n)}{n} = \frac{Q_0^C(n)}{n} - c \right\} \xrightarrow{a.s.} \inf_{t \geq 0} \{c\mu t = \psi_0^C - c\} = \frac{(\psi_0^C - c)^+}{c\mu}.$$

Then, by re-expressing the sum of indicators as

$$\frac{1}{n} \sum_{i=1}^{cn \wedge Q_0^C(n)} \mathbf{1}\{S_i + \tau_n > t\} = \frac{cn \wedge Q_0^C(n)}{n} \left( \frac{1}{cn \wedge Q_0^C(n)} \sum_{i=1}^{cn \wedge Q_0^C(n)} \mathbf{1}\{S_i + \tau_n > t\} \right),$$

we can furthermore observe through the law of large numbers that

$$\frac{cn \wedge Q_0^C(n)}{n} \left( \frac{1}{cn \wedge Q_0^C(n)} \sum_{i=1}^{cn \wedge Q_0^C(n)} \mathbf{1}\{S_i + \tau_n > t\} \right) \xrightarrow{a.s.} (\psi_0^C \wedge c) e^{-\mu \left( t - \frac{(\psi_0^C - c)^+}{c\mu} \right)}.$$

Hence, we have shown convergence to the inter-jump dynamics for the initial arrival. We can then note that the convergence of the first jump size follows directly from the assumption on the batch sizes, i.e.  $\frac{B_1(n)}{n} \xrightarrow{D} M_1$ . We now take this convergence as the base case of an inductive proof at each arrival epoch. Moving to the inductive step, we will now assume that the distribution of batch scaled queueing model converges to the  $c$ -threshold storage process at arrival epochs  $1, \dots, k$  for some  $k \in \mathbb{Z}^+$ . Then, let us consider the distribution of the queue up to the next arrival time so we now take  $t$  as  $A_k \leq t < A_{k+1}$ . As in the base case, we can note that the queue length  $Q_t^C(n)$  is equal in distribution to

$$Q_t^C(n) \stackrel{D}{=} \left( Q_{A_k}^C(n) - cn - Z_t^k(n) \vee 0 \right) + \sum_{i=1}^{cn \wedge Q_{A_k}^C(n)} \mathbf{1}\{S_i^k + \tau_n^k > t\},$$

where  $Z_t^k(n)$  is a Poisson process with rate  $cn\mu$  and  $Z_{A_k}^k(n) = 0$  by assumption,  $S_i^k \stackrel{iid}{\sim} \text{Exp}(\mu)$  are independent from  $Z_t^k(n)$ , and  $\tau_n^k = \inf_{t \geq A_k} \{Z_t^k = Q_{A_k}^C(n) - cn\}$ . By the memoryless property of the exponential distribution, we have  $Z_t^k(n)$  and  $\{S_i^k \mid i \in \mathbb{Z}^+\}$  are independent from the history of the queueing process. We can now repeat the same reasoning as in the base case. Because  $\frac{Z_t^k(n)}{n} \xrightarrow{a.s.} c\mu t$  as  $n \rightarrow \infty$ , one can observe that

$$\left( \frac{Q_{A_k}^C(n)}{n} - c - \frac{Z_t^k(n)}{n} \vee 0 \right) \xrightarrow{D} (\psi_{A_k}^C - c - c\mu t \vee 0),$$

due to the inductive assumption that  $\frac{Q_{A_k}^C(n)}{n} \xrightarrow{D} \psi_{A_k}^C$ , and this means that

$$\tau_n^k = \inf_{t \geq A_k} \left\{ \frac{Z_t^k(n)}{n} = \frac{Q_{A_k}^C(n)}{n} - c \right\} \xrightarrow{D} \inf_{t \geq A_k} \{c\mu t = \psi_{A_k}^C - c\} = A_k + \frac{(\psi_{A_k}^C - c)^+}{c\mu}.$$



Hence for the sum of indicators we also find that

$$\frac{cn \wedge Q_{A_k}^C(n)}{n} \left( \frac{1}{cn \wedge Q_{A_k}^C(n)} \sum_{i=1}^{cn \wedge Q_{A_k}^C(n)} \mathbf{1}\{S_i^k + \tau_n^k > t\} \right) \xrightarrow{D} (\psi_{A_k}^C \wedge c) e^{-\mu \left( t - A_k - \frac{(\psi_{A_k}^C - c)^+}{c\mu} \right)},$$

as  $\frac{Q_{A_k}^C(n)}{n} \xrightarrow{D} \psi_{A_k}^C$  by the inductive hypothesis and

$$\frac{1}{cn \wedge Q_{A_k}^C(n)} \sum_{i=1}^{cn \wedge Q_{A_k}^C(n)} \mathbf{1}\{S_i^k + \tau_n^k > t\} \xrightarrow{D} e^{-\mu \left( t - A_k - \frac{(\psi_{A_k}^C - c)^+}{c\mu} \right)},$$

through use of the law of large numbers for the indicator converging to the complementary CDF and by the convergence of  $\tau_n^k$  to  $A_k + (\psi_{A_k}^C - c)^+/c\mu$  that we have just shown. This again matches the inter-jump dynamics of the  $c$ -threshold process: linear drain above the threshold and exponential decay below. Then, at the arrival epoch we have  $\frac{B_{k+1}(n)}{n} \xrightarrow{D} M_{k+1}$  by assumption which means that  $\frac{Q_{A_{k+1}}^C(n)}{n} \xrightarrow{D} \psi_{A_{k+1}}^C$ . Thus, by induction we complete proof.  $\square$

Just as we gave a visual example of the convergence of infinite server queues to shot noise processes in Figure 2.1, we now plot a series of simulated delay model distributions in Figure 2.2 and compare them to a  $c$ -threshold storage process. For this example we suppose that the batch sizes are geometrically distributed with probability of success  $\frac{1}{n}$ , and this yields jumps that are exponentially distributed with unit rate in the batch scaling limit. As an additional example of the limiting threshold dynamics, in Figure 2.3 we plot a simulated scaled queue length sample path along with the calculated storage process values when given the same arrival epochs. One can observe the change in release behavior as the process crosses the capacity level  $c$ . Above  $c$  the content drains linearly, below  $c$  it decays exponentially.

We now turn to the blocking model  $Q_t^B(n)$ . To motivate this final batch scaling, consider the relationship between this model and the infinite server queue. Given that both have exponentially distributed service durations, the rate of departure in either model is  $\mu k$  when there is  $k$  in system. However, while the infinite server model can accept an arriving batch of any size, the blocking model will only admit entities until it reaches its server capacity. Thus, for an arriving batch of size  $B(n)$  at time  $t$  in the  $G^{B_1(n)}/M/cn/cn$  model, the number of admitted entities is  $(B(n) \wedge cn - Q_t^B(n))$ . Taking this as inspiration, we now define the finite capacity storage process  $\psi_t^B$  as

$$\psi_t^B = \psi_0^B + \bar{J}_t - \mu \int_0^t \psi_s^B ds, \quad (2.8)$$

with  $\bar{J}_t \stackrel{D}{=} \sum_{i=1}^{N_t} (M_i \wedge c - \psi_{A_i^-}^B)$  where  $\psi_{A_i^-}^B = \lim_{t \uparrow A_i} \psi_t^B$ . As a consequence of this definition,  $\psi_t^B \leq c$  at all times  $t$ . Just as the departure rate of the blocking queueing model matches the departure rate of the infinite server model on the same states, the release rule of this finite storage process matches the release rule of the shot noise process, which is the corresponding infinite capacity storage process. Furthermore, like the blocking model the finite capacity storage process features an admittance structure

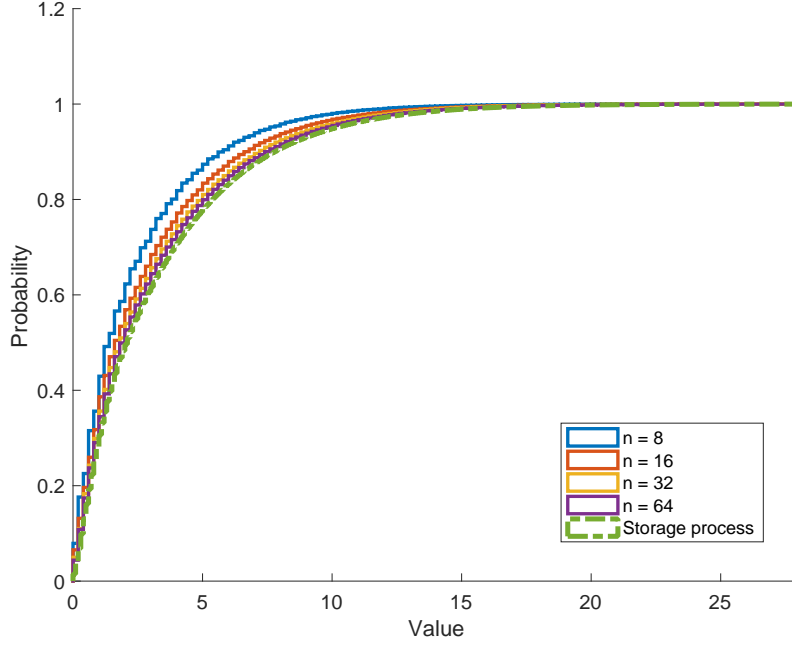


Figure 2.2: Simulated demonstration of convergence in distribution of an  $M^X/M/cn$  queue to a  $c$ -threshold storage process, based on 100,000 replications with  $t = 10$ ,  $\lambda = 3$ ,  $\mu = 2$ ,  $c = 2$ , and  $B_1(n) \sim \text{Geo}(\frac{1}{n})$ .

that depends on its current state. Using the assumption that the initial values of these two processes exist and satisfy  $\frac{Q_0^B(n)}{n} \rightarrow \psi_0^B$ , we now show convergence of the blocking model to the finite storage process in Theorem 2.5.

**Theorem 2.5.** *As  $n \rightarrow \infty$ , the batch scaling of the  $G^X/M/cn/cn$  queue  $Q_t^B(n)$  yields*

$$\frac{Q_t^B(n)}{n} \xrightarrow{D} \psi_t^B, \quad (2.9)$$

*pointwise in  $t \geq 0$ , where  $\psi_t^B$  is a finite storage process as defined in Equation 2.8.*

*Proof.* In a similar manner as in the proof of Theorem 2.4, we will show this convergence by induction on the arrival epochs by considering the inter-jump dynamics as well as the size of each jump. Let  $\{A_k \mid k \in \mathbb{Z}^+\}$  be the sequence of arrival epochs; because of the equivalence of the arrival processes we will not distinguish the epochs by process. As a natural base case we start by studying the process up to the first arrival epoch. Because no entities wait in a blocking model queue by definition, we can express the queue length at time  $t$  where  $0 \leq t < A_1$  as

$$Q_t^B(n) \stackrel{D}{=} \sum_{i=1}^{Q_0^B(n)} \mathbf{1}\{S_i > t\},$$

where  $\{S_i \mid i \in \mathbb{Z}^+\}$  is a sequence of independent random variables that are each equivalent in distribution to the service duration. By the continuous mapping theorem

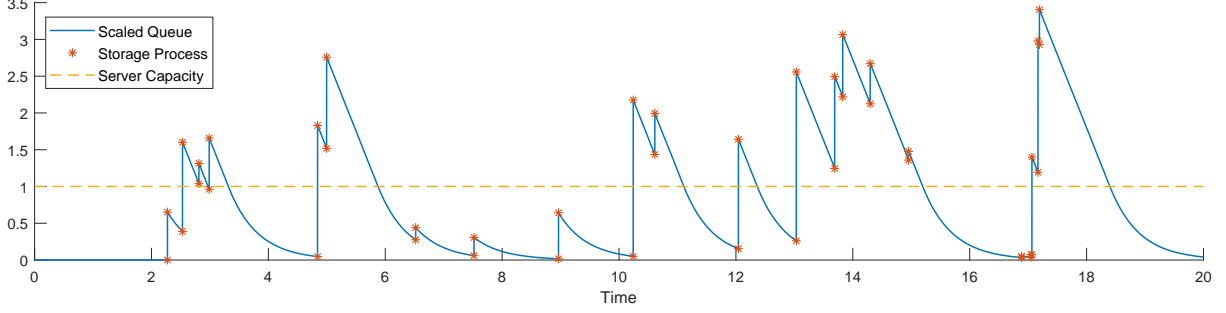


Figure 2.3: A comparison of the simulated scaled queue length process and the calculated storage process sample paths defined on the same arrival process.

and the law of large numbers we can see that

$$\frac{Q_t^B(n)}{n} \stackrel{D}{=} \frac{Q_0^B(n)}{n} \frac{1}{Q_0^B(n)} \sum_{i=1}^{Q_0^B(n)} \mathbf{1}\{S_i > t\} \xrightarrow{a.s.} \psi_0^B e^{-\mu t},$$

as  $e^{-\mu t}$  is the complementary CDF of the exponential distribution. Thus, the inter-jump dynamics of the batch scaled queue converge to the exponential decay of the finite capacity storage process for all time up to the first arrival occurs. What remains to be shown is that the admitted portion of the first batch converges to the jump in the storage process, which we will now show. By letting  $Q_{A_k^-}^B(n)$  be the queue length just before the  $k^{\text{th}}$  batch arrives and letting  $Q_{A_k^+}^B(n)$  be the queue length immediately after, we can write total number of entities admitted from the  $k^{\text{th}}$  batch as  $Q_{A_k^+}^B(n) - Q_{A_k^-}^B(n)$ . Furthermore, we can also note that this quantity will be equal to the minimum of the arriving batch size,  $B_k(n)$ , and the number of available servers,  $cn - Q_{A_k^-}^B(n)$ . Thus at the first arrival epoch we can observe that the total number of admitted entities is such that

$$\frac{1}{n} \left( Q_{A_1^+}^B(n) - Q_{A_1^-}^B(n) \right) = \frac{1}{n} \left( B_1(n) \wedge cn - Q_{A_1^-}^B(n) \right) \stackrel{D}{\Rightarrow} (M_1 \wedge c - \psi_{A_1^-}^B) = \psi_{A_1^+}^B - \psi_{A_1^-}^B,$$

where this follows from the assumed convergence of the batch sequence and of the initial values. Thus, the first admission amount converges to the first jump size and the inductive hypothesis holds in the base case, meaning  $\frac{Q_t^B(n)}{n} \stackrel{D}{\Rightarrow} \psi_t^B$  for  $0 \leq t \leq A_1$ .

We now move to the inductive step and apply similar arguments. As an inductive hypothesis, we assume that the queueing process converges in distribution to the finite storage process up through the first  $k$  arrival times. Like in the base case we start with the behavior between jumps. For time  $t$  such that  $A_k \leq t < A_{k+1}$ , we can express the queue length process as

$$Q_t^B(n) \stackrel{D}{=} \sum_{i=1}^{Q_{A_k}^B} \mathbf{1}\{S_i^k + A_k > t\},$$

where again  $\{S_i^k \mid i \in \mathbb{Z}^+\}$  is a sequence of independent and exponentially distributed random variables with rate  $\mu$  that are also independent from the process history. Then,

using the inductive hypothesis and the law of large numbers we can observe that

$$\frac{Q_t^B(n)}{n} \stackrel{D}{=} \frac{Q_{A_k}^B(n)}{n} \frac{1}{Q_{A_k}^B(n)} \sum_{i=1}^{Q_{A_k}^B(n)} \mathbf{1}\{S_i^k + A_k > t\} \stackrel{D}{\Rightarrow} \psi_{A_k}^B e^{-\mu(t-A_k)}.$$

Because this shows convergence of the inter-jump dynamics on  $A_k \leq t < A_{k+1}$  we now consider the admitted portion of the arriving batch. As discussed in the base case, we know that this amount can be expressed  $Q_{A_{k+1}}^{B+}(n) - Q_{A_{k+1}}^{B-}(n) = (B_{k+1}(n) \vee cn - Q_{A_{k+1}}^{B-}(n))$ . Therefore by the batch sequence convergence and the inductive hypothesis, we can observe that the number of entities admitted from this batch is such that

$$\frac{1}{n} \left( Q_{A_{k+1}}^{B+}(n) - Q_{A_{k+1}}^{B-}(n) \right) \stackrel{D}{\Rightarrow} \left( M_{k+1} \vee c - \psi_{A_{k+1}}^{B-} \right) = \psi_{A_{k+1}}^{B+} - \psi_{A_{k+1}}^{B-},$$

which implies that  $\frac{Q_t^B(n)}{n} \stackrel{D}{\Rightarrow} \psi_t^B$  for all  $t$  on  $A_k \leq t \leq A_{k+1}$ . Hence, we have completed the induction and the proof.  $\square$

*Remark.* An immediate consequence of Theorems 2.3, 2.4, and 2.5 is that simulation of batch arrival queueing systems can be greatly simplified. For large batch sizes, one can simply simulate a storage process, which only requires generating random variables for the arrival epochs and jump sizes; one need not simulate service durations. In the large batch setting, this can deliver substantial savings in computation complexity.

Just as we have visualized the convergence of the infinite server and delay model queues in Figures 2.1 and 2.2, respectively, we plot the analogous demonstration for the blocking model queues and finite capacity storage processes in Figure 2.4. For this example the batches are binomially distributed with number of trials  $n$  and probability of success  $\frac{1}{2}$ , and this yields deterministic jumps of size  $\frac{1}{2}$  in the finite capacity storage process. One can observe that the scaled queue lengths and the finite capacity storage process all lie on the interval  $[0, 2]$ , and that as the batch size grows large the distributions of the queue appear to approach that of the storage process.

As a summary of the storage processes found in the batch scalings shown in the Theorems 2.3, 2.4, and 2.5, recall that we have defined

- i) the shot noise process  $\psi_t$  given by Equation 2.3, which is the batch scaled analog of the infinite server model,
- ii) the  $c$ -threshold storage process  $\psi_t^C$  given by Equation 2.6, which is the batch scaled analog of the delay model,
- iii) the finite capacity storage process  $\psi_t^B$  given by Equation 2.8, which is the batch scaled analog of the blocking model.

The convergences of these three processes are contrasted in the example shown in Figure 2.5. For the sake of comparison, all three simulation scenarios use the same parameter settings: Poisson process arrivals at rate  $\lambda = 5$ , exponential service at rate  $\mu = 2$ , and deterministic batch sizes. For the delay and blocking models,  $c = 3$ . As an informal observation, we can see that the delay queueing models appear to be slightly less visually similar to the limiting  $c$ -threshold storage process than the other two queueing models are to their respective storage process limits, suggesting a somewhat slower rate of convergence for distribution of the delay model in this example.

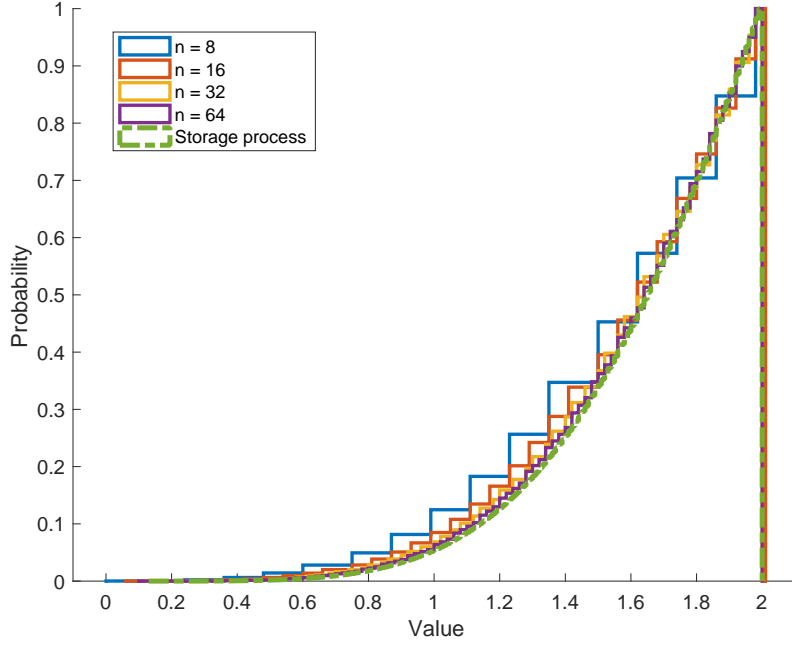


Figure 2.4: Simulated demonstration of convergence in distribution of an  $M^X/M/cn/cn$  queue to a finite capacity storage process, based on 100,000 replications with  $t = 10$ ,  $\lambda = 5$ ,  $\mu = 1$ ,  $c = 2$ , and  $B_1(n) \sim \text{Bin}(n, \frac{1}{2})$ .

In conceptually comparing the processes  $\psi_t^C$  and  $\psi_t^B$ , one can note that each has an inherent reliance on the parameter  $c$ . This quantity will be the focal point of our teleoperations center staffing analysis. By recognizing  $c$  as a ratio between the relative batch size  $n$  and the number of servers needed, in the following section we will use all three of these storage processes to determine the service capacity that is necessary to support an autonomous vehicle teleoperations system.

### 3 Staffing the Teleoperations System

We now observe that we can use the storage process processes found in the preceding section to determine the staffing performance levels of the delay and blocking queueing models with large batch sizes. In the delay model, we want to calculate the probability that the queue is above its capacity, which means that there are jobs waiting to begin service. By use of the batch scaling result, we can see that this is

$$\mathbb{P}(Q_t^C(n) > cn) = \mathbb{P}\left(\frac{Q_t^C(n)}{n} > c\right) \rightarrow \mathbb{P}(\psi_t^C > c),$$

as  $n \rightarrow \infty$  and thus as the relative batch sizes grow large this becomes the probability that  $\psi_t^C$  is above its threshold. Likewise in the blocking model, we want to compute the probability that some portion of an arriving batch is blocked, which means that the sum of the pre-arrival queue length and the incoming batch size exceeds the number



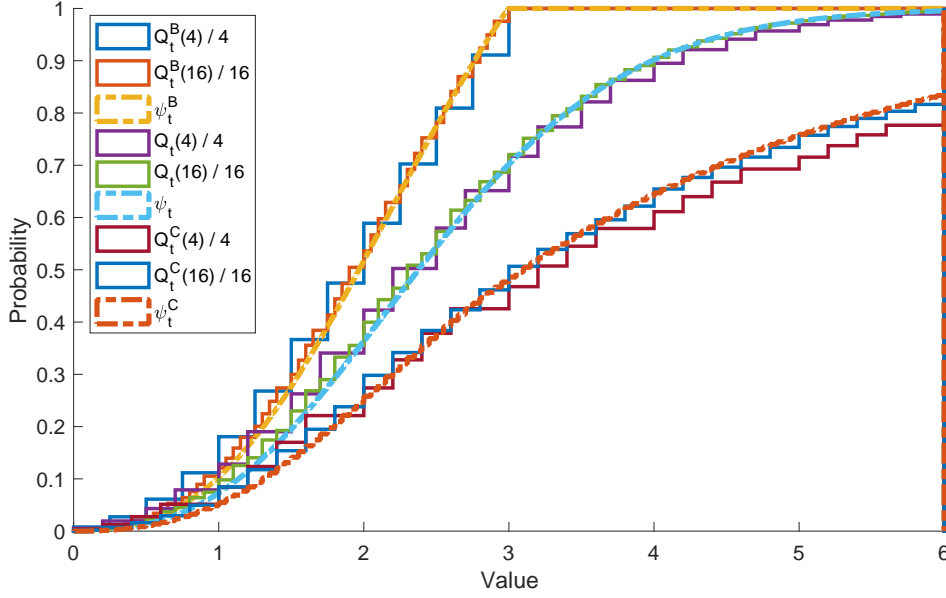


Figure 2.5: Comparison of convergences of Markovian infinite server, delay, and blocking queueing models, based on 100,000 replications with  $t = 10$ ,  $\lambda = 5$ ,  $\mu = 2$ , and  $B_1(n) = n$ , where  $c = 3$  in the delay and blocking models.

of servers. Again we find a connection to the corresponding storage process, as this converges to the probability that the finite storage processes  $\psi_t^B$  is above its capacity as the relative batch size grows large:

$$\mathbb{P}(Q_t^B(n) + B(n) > cn) = \mathbb{P}\left(\frac{Q_t^B(n)}{n} + \frac{B(n)}{n} > c\right) \longrightarrow \mathbb{P}(\psi_t^B + M > c).$$

Since both of these revolve around the quantity  $c$ , let us discuss its interpretations in the queues and in the storage processes. In both the delay and blocking queueing systems,  $c$  is a ratio between the relative batch size  $n$  and the number of servers  $cn$ . So, as  $c$  grows large the number of remote operators at the teleoperations center will be a larger multiple of the batch size. In the  $c$ -threshold and finite capacity storage processes,  $c$  is a threshold level. For the  $c$ -threshold process this is a level that dictates different release rate above and below as shown in Figure 2.3. In the finite capacity model,  $c$  is the capacity of the system; any jump that exceeds this amount will instead just jump to  $c$ .

To study  $\psi_t$ ,  $\psi_t^C$ , and  $\psi_t^B$ , we can draw upon the well-established storage processes literature. To leverage these results, we will hereforward assume that the arrival epoch process  $N_t$  is a Poisson process with rate  $\lambda > 0$ . We note that this Poisson process is only for the times of jumps in the storage process or arrivals in the queue, and the arrival bursts phenomenon is still captured through the batch arrivals, as discussed in Subsection 2.1. Additionally, we will assume that the shot noise process  $\psi_t$  has release rule  $r(x) = \mu x$ , so that this draining of this process mimics that of  $\psi_t^C$  and  $\psi_t^B$ . Following standard stability assumptions for multi-server queueing models we will also suppose  $\lambda \mathbb{E}[B_1(n)] < cn\mu$  for all  $n \in \mathbb{Z}^+$  and we suppose that in the limit we have

$\lambda E[M_1] < c\mu$  as well. Thus, the objects we use to determine the staffing levels will be the storage processes in steady-state. We denote these as  $\psi_\infty$ ,  $\psi_\infty^C$ , and  $\psi_\infty^B$  for the shot noise,  $c$ -threshold, and finite capacity processes, respectively. Then, as a first result from the storage processes literature that we will employ, we cite integral equations for the steady-state densities of  $\psi_\infty$  and  $\psi_\infty^C$  in Lemma 3.1.

**Lemma 3.1.** *The steady-state density of the shot noise process  $f_\infty(\cdot)$  exists and satisfies the integral equation*

$$f_\infty(x) = \frac{\lambda}{x\mu} \int_0^x P(M_1 > x - y) f_\infty(y) dy, \quad (3.1)$$

for all  $x > 0$ . Furthermore, the steady-state density of the  $c$ -threshold storage process  $f_C(\cdot)$  exists and satisfies the integral equation

$$f_C(x) = \frac{\lambda}{(x \wedge c)\mu} \int_0^x P(M_1 > x - y) f_C(y) dy, \quad (3.2)$$

for all  $x > 0$ .

*Proof.* This follows directly from Theorem 5 of Brockwell et al. [6].  $\square$

As a second lemma from the literature we cite a truncation result for the steady-state density of  $\psi_\infty^B$ , which we can view as analogous to several known queueing results. For example, the reversibility of the  $M/M/\infty$  queue implies that truncation yields the stationary distribution of the  $M/M/c/c$  Erlang-B model. This can even be observed in non-reversible models, as the steady-state distribution of a batch arrival blocking model can be obtained via truncating the steady-state distribution of an infinite server queue with batch arrivals. This can be seen as a result of Proposition 2.5 of Daw and Pender [16]. Now in Lemma 3.2 we see that this is also known in the storage process literature, as the density of a finite dam with Poisson process epochs can be found via truncation of a shot noise process.

**Lemma 3.2.** *The steady-state density of the finite capacity storage process  $f_B(\cdot)$  exists and is given by*

$$f_B(x) = \frac{f_\infty(x)}{\int_0^c f_\infty(y) dy}, \quad (3.3)$$

for all  $0 < x \leq c$ , where  $f_\infty(\cdot)$  is the steady-state density of the shot noise process.

*Proof.* See Section 8 of Brockwell [7].  $\square$

These lemmas will now guide our approach to staffing, in which we find the probability of the  $c$ -threshold storage process having excess content  $P(\psi_\infty^C > c)$  and the fraction of all arrivals that have a jump partially blocked in the finite storage process  $P(\psi_\infty^B + M_1 > c)$ . We will refer to these quantities in each context as the exceedance probabilities. We perform this analysis in two different streams. First, in Subsection 3.1 we prove that sums based on Legendre polynomial coefficients and the moment generating function of the shot noise process converges to both exceedance probabilities. This is a general approach that makes no assumptions on the batch/jump size distributions. By comparison in Subsection 3.2 we show that with more assumptions one can often find explicit results for the distributions as a whole and for the sake of example we consider geometric batch sizes, which correspond to exponential marks.

### 3.1 Asymptotic Analysis for General Batch Sizes

To support our general analysis we will now introduce a general technical lemma, which extends Sullivan et al. [43] to a probabilistic context. In Sullivan et al. [43], the authors use shifted, asymmetric Legendre polynomials to produce a sum of exponential functions of  $x \geq 0$  that converges to the indicator function  $\mathbf{1}\{x \leq c\}$  for any constant  $c > 0$ . By use of the dominated convergence theorem, in Lemma 3.3 we generalize this to a sum of moment generating functions of a continuous non-negative random variable. We find convergence to the cumulative distribution function of the random variable, as well as to the expectation of the product between the random variable and the indicator function. Therefore, this lemma provides a method to find this cumulative probability and expectation when one only has access to the moment generating function of a non-negative random variable. This will be paramount to our following general staffing analysis, and because of its generality we believe it may also be of use in other applications. For clarity's sake, we note that the moment generating functions used in this technique are for strictly negative space parameters and thus will exist for all distributions. These functions can thus be viewed as Laplace transforms of the density with real, negative arguments.

**Lemma 3.3.** *Let  $X$  be a non-negative continuous random variable and let  $\mathcal{M}(\cdot)$  be its moment generating function and let  $\mathcal{M}'(\cdot)$  be its first derivative, i.e.  $\mathcal{M}(z) = \mathbb{E}[e^{zX}]$  and  $\mathcal{M}'(z) = \frac{d}{dz}\mathbb{E}[e^{\theta X}]|_{\theta=z}$ . Then, for the sequence  $\{a_k^m \mid m, k \in \mathbb{Z}^+\}$  given by*

$$a_k^m = (-1)^{k+1} \binom{m}{k} \binom{m+k}{k} {}_3F_2\left(k, -m, m+1; 1, k+1; \frac{1}{e}\right), \quad (3.4)$$

*the summation over the products between  $a_k^m$  and  $\mathcal{M}\left(-\frac{k}{c}\right)$  is such that*

$$\lim_{m \rightarrow \infty} \sum_{k=1}^m a_k^m \mathcal{M}\left(-\frac{k}{c}\right) = \mathbb{P}(X \leq c), \quad (3.5)$$

*whereas the summation over the products between  $a_k^m$  and  $\mathcal{M}'\left(-\frac{k}{c}\right)$  is such that*

$$\lim_{m \rightarrow \infty} \sum_{k=1}^m a_k^m \mathcal{M}'\left(-\frac{k}{c}\right) = \mathbb{E}[X \mathbf{1}\{X \leq c\}], \quad (3.6)$$

*for all  $c > 0$ .*

*Proof.* For  $x \geq 0$  and  $m \in \mathbb{Z}^+$ , let the function  $\mathcal{L}_m(x)$  be defined as

$$\mathcal{L}_m(x) = \sum_{k=1}^m a_k^m e^{-\frac{kx}{c}}, \quad (3.7)$$

where each  $a_k^m$  is as given in Equation 3.4. By Sullivan et al. [43], we have that

$$\int_0^\infty (\mathcal{L}_m(x) - \mathbf{1}\{x \leq c\})^2 dx \rightarrow 0,$$

as  $m \rightarrow \infty$ , which implies that  $\mathcal{L}_m(x) \rightarrow \mathbf{1}\{x \leq c\}$  pointwise for  $x \in [0, c)$  and  $x \in (c, \infty)$  as  $m \rightarrow \infty$ . Furthermore, from Sullivan et al. [43] we also have that  $\mathcal{L}_m(x)$

can be equivalently expressed

$$\mathcal{L}_m(x) = - \int_0^1 \tilde{P}_m\left(\frac{w}{e}\right) \frac{d}{dw} \tilde{P}_m\left(we^{-\frac{x}{c}}\right) dw, \quad (3.8)$$

where  $\tilde{P}_m(\cdot)$  is a shifted, asymmetric Legendre polynomial defined by

$$\tilde{P}_m(w) = \sum_{k=0}^m \binom{m}{k} \binom{m+k}{k} (-w)^k,$$

for  $w \in [0, 1]$ . For reference, this can be connected to a standard Legendre polynomial  $P_m(\cdot)$  via the transformation  $\tilde{P}_m(w) = P_m(1 - 2w)$ . To employ the dominated convergence theorem, we now bound  $|\mathcal{L}_m(x)|$  as follows. Via the integral definition in Equation 3.8, we can observe that the values of this function at the origin are  $\mathcal{L}_m(0) = 1 + (-1)^{m+1} \tilde{P}_m(1/e)$ , meaning that  $\mathcal{L}_m(0) \in (0, 2)$  for all  $m$ . Hence, we now focus on the quantity when  $x$  is positive. In this case, we can see that

$$\sup_{x>0} \left| \int_0^1 \tilde{P}_m\left(\frac{w}{e}\right) \frac{d}{dw} \tilde{P}_m\left(we^{-\frac{x}{c}}\right) dw \right| \leq \sup_{x>0} \left| \int_0^1 \frac{d}{dw} \tilde{P}_m\left(we^{-\frac{x}{c}}\right) dw \right|,$$

which can be explained as follows. Note  $x$  dictates how much or how little to integrate along  $\frac{d}{dw} \tilde{P}_m(we^{-\frac{x}{c}})$ . That is, at  $x = 0$ , the integral evaluates  $\frac{d}{dw} \tilde{P}_m(w)$  at every point in its domain  $[0, 1]$  but for positive  $x$  the derivative is only evaluated from 0 to  $e^{-\frac{x}{c}}$ . Because we know that the shifted Legendre polynomial is bounded on  $-1 \leq \tilde{P}_m(\cdot) \leq 1$ , the integral on the left hand side is subject to negative values in both  $\tilde{P}_m(w/e)$  and  $\frac{d}{dw} \tilde{P}_m(we^{-\frac{x}{c}})$ , whereas the right hand side only has  $\frac{d}{dw} \tilde{P}_m(we^{-\frac{x}{c}})$ . Note furthermore that  $\tilde{P}_m(w/e)$  and  $\frac{d}{dw} \tilde{P}_m(we^{-\frac{x}{c}})$  cannot match in sign at every  $w \in [0, 1]$ , as  $\tilde{P}_m(w/e)$  is a polynomial of degree  $m$  while  $\frac{d}{dw} \tilde{P}_m(we^{-\frac{x}{c}})$  is a polynomial of degree  $m - 1$ . Thus, any interval that the integral on the left hand side evaluates over can be improved upon in the right hand side by evaluating only on a subinterval in which the derivative is positive, and it does so with a larger value as  $\tilde{P}_m(w/e) \leq 1$ . Integrating on the right hand side now leads us to the simpler form

$$\sup_{x>0} \left| \int_0^1 \frac{d}{dw} \tilde{P}_m\left(we^{-\frac{x}{c}}\right) dw \right| = \sup_{x>0} \left| 1 - \tilde{P}_m\left(e^{-\frac{x}{c}}\right) \right| \leq 2,$$

where the final bound again follows through the observation that  $-1 \leq \tilde{P}_m(\cdot) \leq 1$ . With this bound in hand, to use the dominated convergence theorem we now review the specific convergence from Sullivan et al. [43]. From Sullivan et al. [43], we have that  $\mathcal{L}_m(x) \rightarrow \mathbf{1}\{x \leq c\}$  pointwise for  $x \in [0, c)$  and  $x \in (c, \infty)$ . At the point of discontinuity in the indicator function at  $x = c$ , it can be observed that  $\mathcal{L}_m(c) \rightarrow \frac{1}{2}$  as  $m \rightarrow \infty$ . Because the random variable  $X$  is assumed to be continuous, the singleton  $\{c\}$  is of measure 0 and thus  $\mathcal{L}_m(x) \rightarrow \mathbf{1}\{x \leq c\}$  almost everywhere, justifying use of the dominated convergence theorem. Using this, we now have that

$$\mathbb{E}[\mathcal{L}_m(X)] \rightarrow \mathbb{E}[\mathbf{1}\{X \leq c\}] = \mathbb{P}(X \leq c) \quad \text{and} \quad \mathbb{E}[X \mathcal{L}_m(X)] \rightarrow \mathbb{E}[X \mathbf{1}\{X \leq c\}],$$

as  $m \rightarrow \infty$ . Using the definition of  $\mathcal{L}_m(x)$  in Equation 3.7 and linearity of expectation, one can write

$$\mathbb{E}[\mathcal{L}_m(X)] = \sum_{k=1}^m a_k^m \mathbb{E}\left[e^{-\frac{kX}{c}}\right] \quad \text{and} \quad \mathbb{E}[X \mathcal{L}_m(X)] = \sum_{k=1}^m a_k^m \mathbb{E}\left[X e^{-\frac{kX}{c}}\right],$$

and by observing that  $\mathcal{M}'\left(-\frac{k}{c}\right) = \mathbb{E}\left[Xe^{-\frac{kX}{c}}\right]$ , we complete the proof.  $\square$

It is worth noting that the batch scalings enable us to use this lemma, as the storage processes satisfy the required condition of continuous support but the queueing models do not. With this lemma in hand, we can now find expressions for the exceedance probabilities in the  $c$ -threshold and finite capacity models. For each case, we will draw upon the tractability of the shot noise process and then convert the findings into the two related cases by use of these Legendre sum forms and the results from the storage processes literature. In Theorem 3.4, we find the threshold exceedance probability for  $\psi_\infty^C$  by expressing the truncated mean of the shot noise process  $\psi_\infty$  as the limiting object of the ratio of two sums from Lemma 3.3 and equating it to the truncated mean of the  $c$ -threshold storage process via Lemma 3.1.

**Theorem 3.4.** *The threshold exceedance probability for  $\psi_\infty^C$  is given by the limit*

$$\mathbb{P}(\psi_\infty^C > c) = \lim_{m \rightarrow \infty} \frac{\frac{\lambda}{\mu} \mathbb{E}[M_1] - \sigma_{m,c}^{(C)}}{c - \sigma_{m,c}^{(C)}}, \quad (3.9)$$

where for  $m \in \mathbb{Z}^+$  and  $c$  as the capacity threshold,  $\sigma_{m,c}^{(C)}$  is given by

$$\sigma_{m,c}^{(C)} = \sum_{k=1}^m \frac{c\lambda}{\mu k} \left(1 - \mathbb{E}\left[e^{-\frac{k}{c}M_1}\right]\right) \frac{a_k^m e^{-\lambda \int_0^\infty \left(1 - \mathbb{E}\left[e^{-\frac{k}{c}M_1 e^{-\mu x}}\right]\right) dx}}{\sum_{i=1}^m a_i^m e^{-\lambda \int_0^\infty \left(1 - \mathbb{E}\left[e^{-\frac{i}{c}M_1 e^{-\mu x}}\right]\right) dx}}, \quad (3.10)$$

with  $a_k^m$  as defined in Equation 3.4.

*Proof.* To begin, we first observe that the mean of the storage process at time  $t \geq 0$  is given by the solution to the differential equation

$$\frac{d}{dt} \mathbb{E}[\psi_t^C] = \lambda \mathbb{E}[M_1] - \mu \mathbb{E}[\psi_t^C \wedge c],$$

as found via the infinitesimal generator of the process. This then leads us to observe that in steady-state the expected value of the minimum of the process content and the server capacity is  $\mathbb{E}[\psi_\infty^C \wedge c] = \frac{\lambda}{\mu} \mathbb{E}[M_1]$ . This same expectation can also be expressed through conditioning as

$$\mathbb{E}[\psi_\infty^C \wedge c] = c \mathbb{P}(\psi_\infty^C > c) + \mathbb{E}[\psi_\infty^C \mid \psi_\infty^C \leq c](1 - \mathbb{P}(\psi_\infty^C > c)),$$

and thus by setting these two expressions equal to one another we find that

$$\mathbb{P}(\psi_\infty^C > c) = \frac{\frac{\lambda}{\mu} \mathbb{E}[M_1] - \mathbb{E}[\psi_\infty^C \mid \psi_\infty^C \leq c]}{c - \mathbb{E}[\psi_\infty^C \mid \psi_\infty^C \leq c]}. \quad (3.11)$$

Although we do not know this truncated mean of  $\psi_\infty^C$  in closed form, we can observe that

$$\mathbb{E}[\psi_\infty^C \mid \psi_\infty^C \leq c] = \mathbb{E}[\psi_\infty^B] = \mathbb{E}[\psi_\infty \mid \psi_\infty \leq c],$$

because the integral equations of the three process truncated densities are equivalent for all  $x \in (0, c]$ , as can be observed through Lemmas 3.1 and 3.2. Now, by total probability we can recognize that

$$\mathbb{E}[\psi_\infty \mid \psi_\infty \leq c] = \frac{\mathbb{E}[\psi_\infty \mathbf{1}\{\psi_\infty \leq c\}]}{\mathbb{P}(\psi_\infty \leq c)}.$$



For  $m \in \mathbb{Z}^+$ , we now define the quantities  $\sigma_{m,c}^{(1)}$  and  $\sigma_{m,c}^{(2)}$  as

$$\sigma_{m,c}^{(1)} = \sum_{k=1}^m a_k^m e^{-\lambda \int_0^\infty (1 - \mathbb{E}[e^{-\frac{k}{c} M_1 e^{-\mu x}}]) dx},$$

$$\sigma_{m,c}^{(2)} = \sum_{k=1}^m \frac{c \lambda a_k^m}{\mu k} \left(1 - \mathbb{E}\left[e^{-\frac{k}{c} M_1}\right]\right) e^{-\lambda \int_0^\infty (1 - \mathbb{E}[e^{-\frac{k}{c} M_1 e^{-\mu x}}]) dx}.$$

Using Theorem 2.3 and Lemma 3.3, we have that  $\sigma_{m,c}^{(1)} \rightarrow \mathbb{P}(\psi_\infty \leq c)$  and  $\sigma_{m,c}^{(2)} \rightarrow \mathbb{E}[\psi_\infty \mathbf{1}\{\psi_\infty \leq c\}]$ . Thus, by substituting  $\sigma_{m,c}^{(C)} = \sigma_{m,c}^{(2)}/\sigma_{m,c}^{(1)}$  into Equation 3.11 and simplifying, we achieve the stated form.  $\square$

By a similar approach, we can also find the probability of an arriving jump exceeding the capacity in the finite storage process. As an aside, we note that we use the subscript 1 simply for notational convenience in  $M_1$ , and we assume that this arriving jump size is an independent draw. Again by use of Lemma 3.3 we find a sum with coefficients based on Legendre polynomials that we connect to this exceedance probability by way of the truncation in Lemma 3.2, which unites the shot noise and finite storage processes.

**Theorem 3.5.** *For  $\psi_\infty^B$ , the fraction of arrival epochs that are at least partially blocked is given by the limit*

$$\mathbb{P}(\psi_\infty^B + M_1 > c) = \lim_{m \rightarrow \infty} \frac{c \mu \sigma_{m,c}^{(B)}}{\lambda}, \quad (3.12)$$

where  $f_M(\cdot)$  is the density of  $M_1$  and where  $\sigma_{m,c}^{(B)}$  is given by

$$\sigma_{m,c}^{(B)} = \sum_{k=1}^m \frac{\lambda}{c \mu} \left(1 - \mathbb{E}\left[e^{-\frac{k}{c} M_1}\right]\right) \frac{a_k^m e^{-\lambda \int_0^\infty (1 - \mathbb{E}[e^{-\frac{k}{c} M_1 e^{-\mu x}}]) dx}}{\sum_{i=1}^m a_i^m e^{-\lambda \int_0^\infty (1 - \mathbb{E}[e^{-\frac{i}{c} M_1 e^{-\mu x}}]) dx}}, \quad (3.13)$$

with  $a_k^m$  as defined in Equation 3.4.

*Proof.* By conditioning on the steady-state value of the finite capacity storage process, we have that

$$\mathbb{P}(\psi_\infty^B + M_1 > c) = \int_0^c \mathbb{P}(M_1 > c - y \mid \psi_\infty^B = y) f_B(y) dy = \int_0^c \mathbb{P}(M_1 > c - y) f_B(y) dy,$$

where  $f_B(\cdot)$  is the density of  $\psi_\infty^B$ , as the sequence of jump sizes is independent. Now by Lemmas 3.1 and 3.2, we can further observe that

$$\int_0^c \mathbb{P}(M_1 > c - y) f_B(y) dy = \int_0^c \mathbb{P}(M_1 > c - y) \frac{f_\infty(y)}{\mathbb{P}(\psi_\infty \leq c)} dy = \frac{c \mu f_\infty(c)}{\lambda \mathbb{P}(\psi_\infty \leq c)},$$

with  $f_\infty(\cdot)$  as the density of  $\psi_\infty$ . Then, for  $m \in \mathbb{Z}^+$  let us define  $\sigma_{m,c}^{(1)}$  as

$$\sigma_{m,c}^{(1)} = \sum_{k=1}^m a_k^m e^{-\lambda \int_0^\infty (1 - \mathbb{E}[e^{-\frac{k}{c} M_1 e^{-\mu x}}]) dx},$$

where we can further note that

$$\frac{\partial}{\partial c} \sigma_{m,c}^{(1)} = \sum_{k=1}^m \frac{\lambda a_k^m}{c\mu} \left( 1 - \mathbb{E} \left[ e^{-\frac{k}{c} M_1} \right] \right) e^{-\lambda \int_0^\infty \left( 1 - \mathbb{E} \left[ e^{-\frac{k}{c} M_1 e^{-\mu x}} \right] \right) dx}.$$

Now through use of Theorem 2.3 and Lemma 3.3, we have that  $\sigma_{m,c}^{(1)} \rightarrow \mathbb{P}(\psi_\infty \leq c)$  and by Theorem 7.17 of Rudin [41] we can further observe that  $\frac{\partial}{\partial c} \sigma_{m,c}^{(1)} \rightarrow f_\infty(c)$ . By combining these functions and simplifying, we achieve the stated result.  $\square$

Through the well-known Poisson arrivals see time averages (PASTA) principle, the expression in Theorem 3.5 is both equal to the steady-state probability that the finite storage process is in a state in which an arrival would exceed the capacity and equal to the fraction of all arrival epochs in which some portion of the jump exceeds the capacity [46]. Before moving forward, we note that this subsection has been concerned with the analytic techniques that yield these exceedance probabilities and we have not yet specifically discussed the numerical implementation of these methods. These numerics are the focus of Section 4, in which we describe how to use these ideas in practice and demonstrate their performance.

## 3.2 Exact Analysis for Geometrically Distributed Batches

As an example of an approach to this staffing problem under more specific assumptions, in this subsection we will suppose that the batch size distribution in the queueing models is geometric, i.e. we let  $B_1(n) \sim \text{Geo}(\frac{\alpha}{n})$  for some  $\alpha > 0$ . From Proposition 2.1, we know that one source of such batch distributions is sudden, external stimuli or shocks to the system. We can observe that having geometrically distributed batch sizes implies that the jumps in the storage process will be exponentially distributed, as

$$\mathbb{E} \left[ e^{\frac{\theta}{n} B_1(n)} \right] = \frac{\frac{\alpha}{n}}{1 - \left( 1 - \frac{\alpha}{n} \right) e^{\frac{\theta}{n}}} = \frac{\alpha}{\alpha e^{\frac{\theta}{n}} - n \left( e^{\frac{\theta}{n}} - 1 \right)} \rightarrow \frac{\alpha}{\alpha - \theta} = \mathbb{E} \left[ e^{\theta M_1} \right],$$

with  $M_1 \sim \text{Exp}(\alpha)$ . In this situation, the assumed stability condition simplifies to  $\lambda < \alpha c \mu$ . As is often the case for exponential random variables, we will find that this leads to significant tractability. Thus, throughout this section we will use the assumption that  $M_1 \sim \text{Exp}(\alpha)$  together with Lemmas 3.1 and 3.2 to find the steady-state densities of  $\psi_\infty$ ,  $\psi_\infty^C$ , and  $\psi_\infty^B$  in closed form. The assumption of exponential marks will be explicitly stated at the beginning of each statement for clarity's sake. Because the shot noise process will again be the cornerstone for the  $c$ -threshold and finite storage processes, we begin by showing that its steady-state value is gamma distributed.

**Proposition 3.6.** *Suppose that  $M_1 \sim \text{Exp}(\alpha)$ . Then,  $\psi_\infty \sim \text{Gamma}(\frac{\lambda}{\mu}, \alpha)$ .*

*Proof.* By Lemma 3.1, we know that for all  $x > 0$  the density  $f_\infty(x)$  will satisfy the integral equation

$$x f_\infty(x) = \frac{\lambda}{\mu} e^{-\alpha x} \int_0^x e^{\alpha y} f_\infty(y) dy.$$

By taking the derivative of each side with respect to  $x$  and simplifying, we find the ordinary differential equation

$$f'_\infty(x) = \frac{1}{x} \left( \frac{\lambda}{\mu} - 1 \right) f_\infty(x) - \alpha f_\infty(x),$$

which yields a solution of  $f_\infty(x) = k_1 e^{-\alpha x} x^{\frac{\lambda}{\mu}-1}$  for some constant  $k_1$ . By requiring that  $\int_0^\infty f_\infty(x) dx = 1$  and solving for the normalizing constant  $k_1$ , we find the density of a Gamma  $\left(\frac{\lambda}{\mu}, \alpha\right)$  random variable.  $\square$

Using this same technique, we can also derive the steady-state density of the  $c$ -threshold storage process  $\psi_\infty^C$ . In this case, we find in Proposition 3.7 that the threshold release rule manifests itself as a piecewise stationary density. In particular, the shape of the distribution below the threshold is proportional to a gamma distribution like what was shown in Proposition 3.6 and above the threshold the density is proportional to an exponential distribution. We can note that this then resembles the conditional distribution of the conditional waiting time in an  $M/M/c$  queue and the conditional distribution of the workload process in an  $M/M/1$  queue, which is one of the classic connections between queues and storage (or dam) processes with linear drain; see for example [37]. Thus, just as a multiserver queue can be seen as a hybrid between an infinite server queue and a single server queue, the  $c$ -threshold storage process can be connected to the storage processes corresponding to the infinite and single server queues, and the structure of each can be plainly observed in the steady-state density of  $\psi_\infty^C$  under these assumptions.

**Proposition 3.7.** *Suppose that  $M_1 \sim \text{Exp}(\alpha)$ . Then,  $\psi_\infty^C$  has probability density function given by*

$$f_C(x) = \begin{cases} \frac{\alpha^{\lambda/\mu} (\alpha c \mu - \lambda) e^{-\alpha x} x^{\frac{\lambda}{\mu}-1}}{(\alpha c \mu - \lambda) \Gamma\left(\frac{\lambda}{\mu}\right) - \alpha c \mu \Gamma\left(\frac{\lambda}{\mu}, \alpha c\right) + \mu \Gamma\left(\frac{\lambda}{\mu} + 1, \alpha c\right)} & 0 \leq x \leq c, \\ \frac{\left(\alpha - \frac{\lambda}{c\mu}\right) \left(\mu \Gamma\left(\frac{\lambda}{\mu} + 1, \alpha c\right) - \lambda \Gamma\left(\frac{\lambda}{\mu}, \alpha c\right)\right) e^{-\left(\alpha - \frac{\lambda}{c\mu}\right)(x-c)}}{(\alpha c \mu - \lambda) \Gamma\left(\frac{\lambda}{\mu}\right) - \alpha c \mu \Gamma\left(\frac{\lambda}{\mu}, \alpha c\right) + \mu \Gamma\left(\frac{\lambda}{\mu} + 1, \alpha c\right)} & x > c. \end{cases} \quad (3.14)$$

*Proof.* From the integral equation given in Lemma 3.1, we can note that the density  $f_C(x)$  satisfies

$$x f_C(x) e^{\alpha x} = \frac{\lambda}{\mu} \int_0^x e^{\alpha y} f_C(y) dy,$$

for  $x \leq c$ , which we have seen yields  $f_C(x) = k_1 e^{-\alpha x} x^{\frac{\lambda}{\mu}-1}$  for some constant  $k_1$  through the proof of Proposition 3.6. Similarly for  $x > c$ , Lemma 3.1 also implies that

$$f_C(x) e^{\alpha x} = \frac{\lambda}{c\mu} \int_0^x e^{\alpha y} f_C(y) dy,$$

and thus this first derivative satisfies the equation

$$f'_C(x) = -\left(\alpha - \frac{\lambda}{c\mu}\right) f_C(x).$$

By consequence,  $f_C(x) = k_2 e^{-(\alpha - \frac{\lambda}{c\mu})x}$  for  $x > c$  and some constant  $k_2$ . To solve for  $k_1$  and  $k_2$ , we can use the fact that the density must integrate to 1 to observe

$$1 = \int_0^\infty f_C(x) dx = k_1 \alpha^{-\frac{\lambda}{\mu}} \left( \Gamma\left(\frac{\lambda}{\mu}\right) - \Gamma\left(\frac{\lambda}{\mu}, \alpha c\right) \right) + \frac{k_2}{\alpha - \frac{\lambda}{c\mu}} e^{-(\alpha - \frac{\lambda}{c\mu})c}.$$

Similarly, because  $E[\phi_\infty^C \wedge c] = \frac{\lambda}{\mu} E[M_1] = \frac{\lambda}{\alpha\mu}$  as seen in the proof of Theorem 3.4, we can also note that

$$\frac{\lambda}{\alpha\mu} = \int_0^\infty (x \wedge c) f_C(x) dx = k_1 \alpha^{-\frac{\lambda}{\mu}-1} \left( \Gamma\left(\frac{\lambda}{\mu} + 1\right) - \Gamma\left(\frac{\lambda}{\mu} + 1, \alpha c\right) \right) + \frac{ck_2}{\alpha - \frac{\lambda}{c\mu}} e^{-(\alpha - \frac{\lambda}{c\mu})c}.$$

This now gives us a system of linear equations of  $k_1$  and  $k_2$ . By solving and simplifying, we achieve the stated form.  $\square$

As a direct consequence of having the steady-state density of  $\psi_\infty^C$  in closed form, we can find an explicit expression for the exceedance probability for this  $c$ -threshold model.

**Corollary 3.8.** *Suppose that  $M_1 \sim \text{Exp}(\alpha)$ . Then, the threshold exceedance probability for  $\psi_\infty^C$  is given by*

$$P(\psi_\infty^C > c) = \frac{\mu \Gamma\left(\frac{\lambda}{\mu} + 1, c\alpha\right) - \lambda \Gamma\left(\frac{\lambda}{\mu}, c\alpha\right)}{(\alpha c\mu - \lambda) \Gamma\left(\frac{\lambda}{\mu}\right) - \alpha c\mu \Gamma\left(\frac{\lambda}{\mu}, c\alpha\right) + \mu \Gamma\left(\frac{\lambda}{\mu} + 1, c\alpha\right)}. \quad (3.15)$$

For the finite storage process  $\psi_\infty^B$ , we will now derive its steady-state density by use of the density for  $\psi_\infty$  in Proposition 3.6 and the truncation equation given in Lemma 3.2. Thus, as we have found that the shot noise process steady-state is equivalent to a gamma random variable, we find in Proposition 3.9 that we can view the resulting density for  $\psi_\infty^B$  as a truncated gamma distribution.

**Proposition 3.9.** *Suppose that  $M_1 \sim \text{Exp}(\alpha)$ . Then,  $\psi_\infty^B$  has probability density function given by*

$$f_B(x) = \frac{\alpha^{\frac{\lambda}{\mu}} x^{\frac{\lambda}{\mu}-1} e^{-\alpha x}}{\Gamma\left(\frac{\lambda}{\mu}\right) - \Gamma\left(\frac{\lambda}{\mu}, \alpha\right)}, \quad (3.16)$$

for all  $0 < x \leq c$ .

*Proof.* By Proposition 3.6, we know that the shot noise process is gamma distributed in steady-state, i.e. it has a density that is proportional to  $e^{-\alpha x} x^{\frac{\lambda}{\mu}-1}$ . By Proposition 3.2, we can normalize this expression so that  $\int_0^c f_B(x) dx = 1$ , and this yields the stated form.  $\square$

Again as an immediate consequence of having an explicit expression for the density of the finite dam content process, we can solve for the probability that an arrival will exceed the finite storage process capacity in closed form.

**Corollary 3.10.** *Suppose that  $M_1 \sim \text{Exp}(\alpha)$ . Then, the capacity exceedance probability for  $\psi_\infty^B$  is given by*

$$\mathbb{P}(\psi_\infty^B + M_1 > c) = \frac{(\alpha c)^{\frac{\lambda}{\mu}} e^{-\alpha c}}{\frac{\lambda}{\mu} \left( \Gamma\left(\frac{\lambda}{\mu}\right) - \Gamma\left(\frac{\lambda}{\mu}, c\alpha\right) \right)}. \quad (3.17)$$

Through Corollary 3.10, it can be seen that one can solve for a target  $c$  in terms of a Lambert-W function when given a target exceedance probability. We also note that the PASTA principle applies here just as it did for Theorem 3.5, and so this exceedance probability can be interpreted as both the fraction of all arrivals that exceed capacity and the probability that the process is in a state in which an arrival would exceed capacity.

## 4 Numerical Experiments

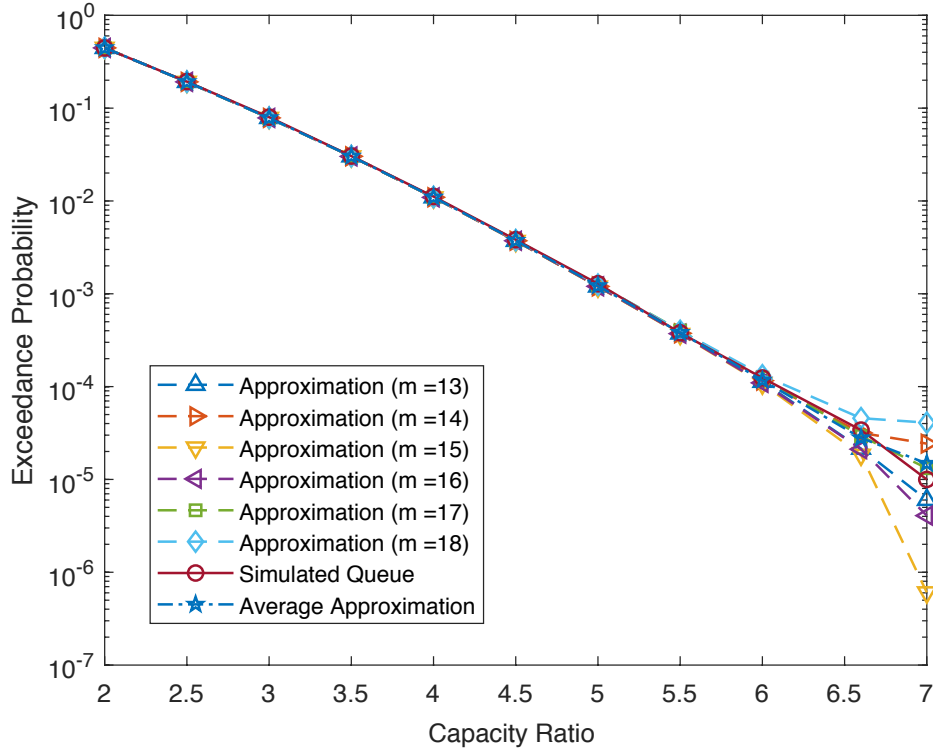


Figure 4.1: Comparison of Legendre approximations and the empirical exceedance probability in a simulated queue with fixed size batches of size  $n = 100$ ,  $\lambda = 3$ , and  $\mu = 2$ .

As an opening numerical discussion, let us demonstrate how we perform approximate implementations of the expressions in Theorems 3.4 and 3.5 as based on the Legendre exponential forms given in Lemma 3.3. As an initial observation, we can note that as  $m$  grows large, calculations of the coefficients given in Equation 3.4 become subject to numerical inaccuracies such as overflow due to the large binomial

coefficients. While this could potentially be assuaged by use of Stirling’s approximation or something similar, in our numerical experiments we have seen that this may not be necessary for strong performance. However, we can note that the convergences in these results need not be monotone so we will not simply take the expression for the largest  $m$  before numerical instability is observed. To explain through example, we will calculate the empirical exceedance probability in the delay queueing model via simulation and compare it to various approximate Legendre sums. Based on Theorem 3.4, we have that

$$\mathbb{P}(Q_\infty^C(n) > cn) \approx \mathbb{P}(\psi_\infty^C > c) \approx \frac{\frac{\lambda}{\mu} \mathbb{E}[M_1] - \sigma_{m,c}^{(C)}}{c - \sigma_{m,c}^{(C)}},$$

and so we will consider candidate  $m$  values, which we plot in Figure 4.1.

As one can see, for relatively small values of  $m$  the approximation performs quite well, as the simulated values and the approximation are virtually indistinguishable before the true probability is approximately of order  $10^{-5}$ . However, if desired we can improve this further by taking the average among the candidate approximations. We can see that this does well in this example, and we can quickly show it will do no worse than the worst individual approximation. For  $p$  as the true probability and  $p_{\sigma_m}$  as the approximation at  $m$ , by the triangle inequality we have that

$$\left| \sum_{k=m_0}^{m_1} \frac{p_{\sigma_k}}{m_1 - m_0 + 1} - p \right| = \left| \sum_{k=m_0}^{m_1} \frac{p_{\sigma_k} - p}{m_1 - m_0 + 1} \right| \leq \sum_{k=m_0}^{m_1} \frac{|p_{\sigma_k} - p|}{m_1 - m_0 + 1} \leq \max_{m_0 \leq k \leq m_1} |p_{\sigma_k} - p|.$$

Thus, a loose description of an approximation heuristic based on these Legendre limits is as follows: compute multiple candidate approximations, remove clear errors caused by numerical instabilities and pre-convergence gaps, and take the average of the remaining candidates. While our experiments suggest that this simple approach does well, we can note that it could be possible to develop more sophisticated numerical approximations based on these limits and we find this to be an interesting direction of future research.

In addition to comparing performance of these methods to simulated values, we can also use them to calculate staffing levels as based on public driving data. Using the 2018 California disengagement reports, GM Cruise LLC [21] and Waymo LLC [45], and the 2017 National Household Travel Survey [18], we find the number of staffing agents needed to support driverless a fleet of driverless vehicles in the ten US metropolitan areas with the most annual miles driven. To calculate the arrival rate we use Waymo’s industry leading 2018 disengagement rate, 1 human takeover per 11,000 miles driven, a 10% penetration rate of driverless vehicles on the road, and an assumption that the peak traffic hour contains 20% of the daily total for each city. For a target exceedance probability of 0.001 and a mean service duration of 1 minute, we calculate the ratio of the staffing level to the mean batch size,  $c$ , in Table 4.1.

One can note that in the traditional notions of blocking and delay probability for the classical  $M/M/c/c$  and  $M/M/c$  models, the number of servers needed to achieve a blocking probability target is typically less than the number needed to achieve the same target for delay probability. This is due to the fact that entities wait in the delay model. However, although this modeling difference still holds in the batch arrival setting we see the opposite relationship taking place in Table 4.1. Because the definition of blocking probability used in Section 3 is that *any* part of the batch is blocked, rather than

Table 4.1: Ratio of the number of remote operators to the relative batch size as calculated for the ten largest U.S. metropolitan areas.

	Metropolitan Area	Annual miles driven (MM)	Disengagement rate (Hourly)	Operator to batch size ratio (Delay)	Operator to batch size ratio (Blocking)
1.	New York, NY	93,512	465.8	15.4	17.2
2.	Los Angeles, CA	71,791	357.6	12.5	13.5
3.	Dallas, TX	50,231	250.2	9.7	10.5
4.	Chicago, IL	49,348	245.8	9.5	10.4
5.	Atlanta, GA	42,547	211.9	8.6	9.5
6.	Houston, TX	42,431	211.4	8.6	9.5
7.	Washington, DC	41,199	205.2	8.5	9.3
8.	Minneapolis, MN	34,540	172.1	7.6	8.4
9.	Philadelphia, PA	32,781	163.3	7.3	8.2
10.	Phoenix, AZ	31,408	156.5	7.1	8.0

the single arrival itself in the solitary arrivals model, achieving a target probability of no blocked batches whatsoever is more stringent than in the model with individual arrivals and in this example it is also more demanding than having the same target probability of the delay system being above capacity. Specifically, in Table 4.1 we can see that the blocking model requires approximately 8%-12% more servers than the delay model needs to achieve the 0.001 target exceedance probability. Therefore in these experiments it takes on the order of 10% more remote operators in the blocking model to deliver the same performance as the delay model.

We can note further that the given ratio of number of servers to batch size, i.e.  $c$ , does not outright depend on the batch size itself and only requires that the batch size is large enough. Thus, the ratios in Table 4.1 hold for any sufficiently large choice of  $n$ . Furthermore, this also shows us that increasing the batch size has a stronger effect on the staffing than increasing the arrival rate does. As one can observe in Table 4.1, the operator to batch size ratio does not increase linearly with the annual miles driven (which is proportional to the arrival rate of support requests or disengagements). For example, the number of miles driven each year in the Minneapolis metropolitan area is roughly half of how many miles are driven in the L.A. area each year (34.5B to 71.8B), yet the resulting ratios of operators to batch size do not exhibit the same relationship (7.6 to 12.5). However, if one considers a doubled batch size rather than a doubled arrival rate, the number of operators needed does truly double. Hence, the relationship between the rate of requests and the number of remote operators is sublinear, whereas the batch size and the number of remote operators are strictly linearly related. This emphasizes one of the key ideas behind our batch-driven work: bursts of arrivals have a pronounced impact on the teleoperations system, particularly when they happen rapidly, and thus they must be addressed.

As a final experiment, we plot the number of servers needed to achieve a 0.001 exceedance probability in both the blocking and delay models as the service rate  $\mu$  increases with the arrival rate fixed at  $\lambda = 250$  disengagements per hour, which is approximately equal to the average of the arrival rates for the ten largest U.S. metro areas. This serves as a comparison between the look-ahead assistance and real-time



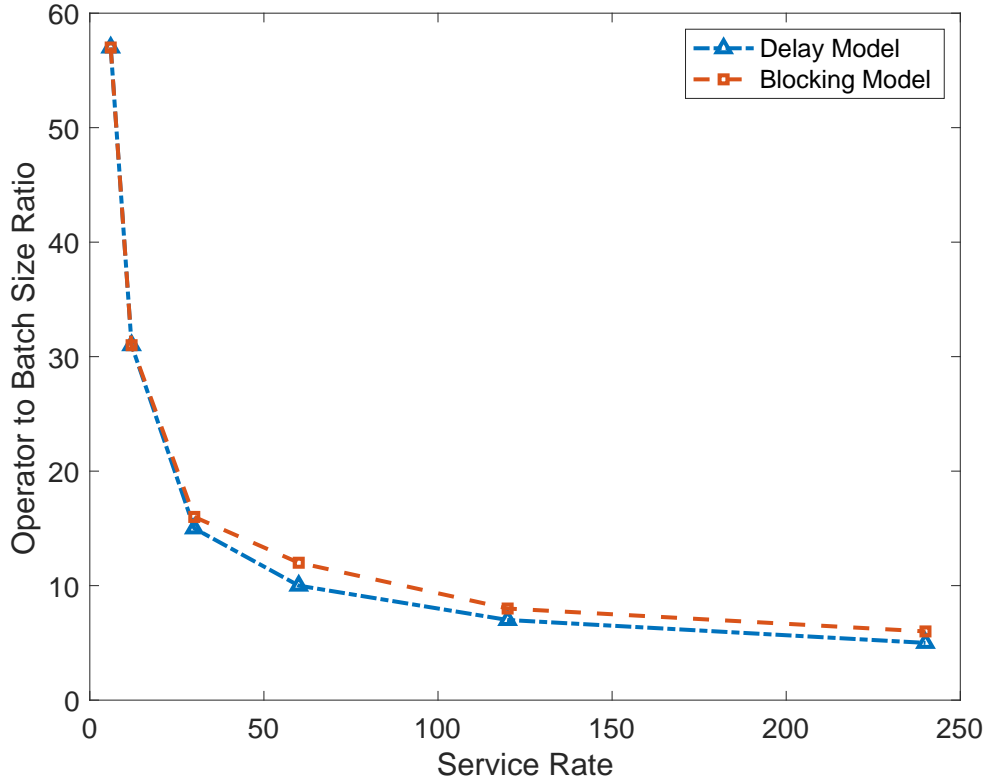


Figure 4.2: Comparison of the operator to batch ratio  $c$  needed to achieve exceedance probability below 0.001 as the service rate  $\mu$  increases when assuming Poisson process arrivals at rate  $\lambda = 250$  disengagements per hour.

operation services. While the human-in-the-loop AI will likely require very fast service in order to keep pace with when the vehicle needs the results, the real-time operation may be longer service as the agent may need to control the vehicle for an extended period of time. We can see that when the service rate  $\mu = 240$  tasks per hour, or an average of 15 seconds per task, the system requires having approximately 6 times as many servers as there are jobs in batches, but when the service rate is  $\mu = 6$  tasks per hour, or an average of 10 minutes per task, the system needs almost 60 times as many agents as there are jobs in a batch.

## 5 Conclusion, Discussion, and Future Work

In this paper we have studied the staffing performance of a teleoperations system for autonomous vehicles. We model this modern service system as a queue with batch arrivals, as we show that batches capture bursts of arrivals as caused by both rapid self-excitement and sudden external shocks. Through these batches, we connect the queueing models to storage processes through novel batch scaling results. Through storage processes, we are able to calculate the probability of the system exceeding capacity, which drives our staffing methodology. We are able to compute these quantities

by leveraging the storage processes literature and introducing a technical lemma that connects sums of evaluations of the moment generating function to quantities such as the cumulative distribution function and the expectation of a random variable multiplied by an indicator function. Through our numerical experiments, we have both validated these analytic results and uncovered interesting relationships. In particular, we have verified the intuition that the size of the batches (or even rapid bursts) of arrivals has more impact on a system’s performance than the arrival rate does.

We believe that there are a variety of opportunities for directly related future work. For example, we are also interested in studying networks of teleoperations centers that support different coverage regions, in which cars may frequently cross into different areas of support. Additionally, we would like to investigate how types affect this teleoperations system, as in practice there may be both different classes of jobs and different skill sets of remote operators. In this case, we can draw upon queueing results such as in Gurvich and Whitt [22, 23], Adan et al. [4], Adan and Weiss [3]. There are also many generalizations of this paper’s results that we are interested in pursuing, such as involving slower acting self-excitement and external stimuli or incorporating non-stationary arrival rates. As another potential direction of work, we could seek to extend the storage processes literature that we have used here. For example, we are interested in using something such as a lack of bias assumption to extend some Poisson based results to non-Poisson settings Melamed and Whitt [35]. We also believe that there is opportunity for clever numerical implementations of the sums in Lemma 3.3, as we discuss briefly in Section 4. Finally, we also intend to investigate different batch scalings of these models and we remain interested in extending these scalings to other related systems.

As a closing comment, we note that this work is only among the first steps in planning and managing a driverless vehicle teleoperation system and many important questions remain across a variety of different disciplines. For example, the look-ahead service requires sophisticated pairings of artificial intelligence and human expertise and this will necessitate careful study and attention to detail to be implemented at scale. Furthermore, this service system asks a great deal of its remote operators, and the profession of repeatedly performing high stakes driving tasks is certainly strenuous enough to prompt study of how to manage this cognitive load. Additionally, there are of course challenges in the design of the communication system supporting this center and there are questions on how to structure the market of the teleoperations services. Because of the variety of the relevant issues, these teleoperations centers pose questions that are not just important and intriguing, but also ones that well suited to the breadth of the operations research community and we hope that this marks the beginning of wide study of teleoperations systems for autonomous vehicles in OR.

## Acknowledgements

This work is partially sponsored by the US DOT Center for Connected and Automated Vehicles (CCAT) based at the University of Michigan’s Transportation Research Institute. We acknowledge the generous support of the National Science Foundation (NSF) for Andrew Daw’s NSF Graduate Research Fellowship under grant DGE-1650441. Additionally, we are grateful to Prof. Walter Lasecki at the University of Michigan for helpful discussions in forming the initial model and identifying the problem scope.

## References

- [1] Preliminary Report Highway: HWY18MH010. *National Transportation Safety Board*, 2018. URL <https://www.nts.gov/investigations/AccidentReports/Pages/HWY18MH010-prelim.aspx>.
- [2] Designated Driver remote operator setup. <https://designateddriver.ai/technology/>, 2019. Accessed: 5/21/2019.
- [3] Ivo Adan and Gideon Weiss. A loss system with skill-based servers under assign to longest idle server policy. *Probability in the Engineering and Informational Sciences*, 26(3):307–321, 2012.
- [4] Ivo Adan, Cor Hurkens, and Gideon Weiss. A reversible Erlang loss system with multitype customers and multitype servers. *Probability in the Engineering and Informational Sciences*, 24(4):535–548, 2010.
- [5] Onno Boxma, Offer Kella, and Michel Mandjes. Infinite-server systems with Coxian arrivals. *Working paper*, 2018. URL <https://scholars.huji.ac.il/sites/default/files/offerkella/files/oom1905181.pdf>.
- [6] Peter J Brockwell, Sidney I Resnick, and Richard L Tweedie. Storage processes with general release rule and additive inputs. *Advances in Applied Probability*, 14(2):392–433, 1982.
- [7] PJ Brockwell. Stationary distributions for dams with additive input and content-dependent release rate. *Advances in Applied Probability*, 9(3):645–663, 1977.
- [8] Lawrence D Burns. Sustainable mobility: a vision of our transport future. *Nature*, 497(7448):181, 2013.
- [9] California Department of Motor Vehicles. Article 3.7 Testing of Autonomous Vehicles. *Title 13, Division 1, Chapter 1*, 2018. URL [https://www.dmv.ca.gov/portal/wcm/connect/a6ea01e0-072f-4f93-aa6c-e12b844443cc/DriverlessAV\\_Adopted\\_Regulatory\\_Text.pdf?MOD=AJPERES](https://www.dmv.ca.gov/portal/wcm/connect/a6ea01e0-072f-4f93-aa6c-e12b844443cc/DriverlessAV_Adopted_Regulatory_Text.pdf?MOD=AJPERES).
- [10] E Cinlar and M Pinsky. On dams with additive inputs and a general release rule. *Journal of Applied Probability*, 9(2):422–429, 1972.
- [11] Daryl J Daley and David Vere-Jones. *An introduction to the theory of point processes: Volume I: Elementary Theory and Methods*. Springer Science & Business Media, 2003.
- [12] Angelos Dassios and Hongbiao Zhao. A dynamic contagion process. *Advances in applied probability*, 43(3):814–846, 2011.
- [13] Alex Davies. The war to remotely control self-driving cars heats up. *Wired*, 2019. URL <https://www.wired.com/story/designated-driver-teleoperations-self-driving-cars/>. Accessed: 6/21/2019.

- [14] Andrew Daw and Jamol Pender. Queues driven by Hawkes processes. *Stochastic Systems*, 8(3):192–229, 2018.
- [15] Andrew Daw and Jamol Pender. The Queue-Hawkes process: Ephemeral self-excitement. *arXiv preprint arXiv:1811.04282*, 2018.
- [16] Andrew Daw and Jamol Pender. On the distributions of infinite server queues with batch arrivals. *Queueing Systems*, 91(3-4):367–401, 2019.
- [17] WF de Graaf, Werner RW Scheinhardt, and Richard J Boucherie. Shot-noise fluid queues and infinite-server systems with batch arrivals. *Performance evaluation*, 116:143–155, 2017.
- [18] Federal Highway Administration. 2017 national household travel survey. *U.S. Department of Transportation, Washington, DC*, 2017. URL <https://nhts.ornl.gov>.
- [19] Xuefeng Gao and Lingjiong Zhu. Functional central limit theorems for stationary Hawkes processes and application to infinite-server queues. *Queueing Systems*, pages 1–46, 2018.
- [20] EN Gilbert and HO Pollak. Amplitude distribution of shot noise. *The Bell System Technical Journal*, 39(2):333–350, 1960.
- [21] GM Cruise LLC. Autonomous vehicle disengagement reports. *California Department of Motor Vehicles*, 2018. URL [https://www.dmv.ca.gov/portal/dmv/detail/vr/autonomous/disengagement\\_report\\_2018](https://www.dmv.ca.gov/portal/dmv/detail/vr/autonomous/disengagement_report_2018).
- [22] Itai Gurvich and Ward Whitt. Queue-and-idleness-ratio controls in many-server service systems. *Mathematics of Operations Research*, 34(2):363–396, 2009.
- [23] Itai Gurvich and Ward Whitt. Service-level differentiation in many-server service systems via queue-ratio routing. *Operations research*, 58(2):316–328, 2010.
- [24] J Michael Harrison and Sidney I Resnick. The stationary distribution and first exit probabilities of a storage process with general release rule. *Mathematics of Operations Research*, 1(4):347–358, 1976.
- [25] J Michael Harrison and Sidney I Resnick. The recurrence classification of risk and storage processes. *Mathematics of Operations Research*, 3(1):57–66, 1978.
- [26] Alan G Hawkes. Spectra of some self-exciting and mutually exciting point processes. *Biometrika*, 58(1):83–90, 1971.
- [27] Haya Kaspi. Storage processes with Markov additive input and output. *Mathematics of operations research*, 9(3):424–440, 1984.
- [28] Haya Kaspi and David Perry. On a duality between a non-Markovian storage/production process and a Markovian dam process with state-dependent input and output. *Journal of Applied Probability*, 26(4):835–844, 1989.

- [29] Philip Koopman and Beth Osyk. Safety argument considerations for public road testing of autonomous vehicles. Technical report, SAE Technical Paper, 2019.
- [30] David T Koops, Onno J Boxma, and MRH Mandjes. Networks of  $\cdot/G/\infty$  queues with shot-noise-driven arrival intensities. *Queueing Systems*, 86(3-4):301–325, 2017.
- [31] DT Koops, Mayank Saxena, OJ Boxma, and Michel Mandjes. Infinite-server queues with Hawkes input. *Journal of Applied Probability*, 55(3):920–943, 2018.
- [32] John A Lane. The central limit theorem for the Poisson shot-noise process. *Journal of applied probability*, 21(2):287–301, 1984.
- [33] Pierre L’Ecuyer, Klas Gustavsson, and Leif Olsson. Modeling bursts in the arrival process to an emergency call center. In *2018 Winter Simulation Conference (WSC)*, pages 525–536. IEEE, 2018.
- [34] Alan Lundgard, Yiwei Yang, Maya L Foster, and Walter S Lasecki. Bolt: Instantaneous crowdsourcing via just-in-time training. In *Proceedings of the 2018 CHI Conference on Human Factors in Computing Systems*, page 467. ACM, 2018.
- [35] Benjamin Melamed and Ward Whitt. On arrivals that see time averages. *Operations Research*, 38(1):156–172, 1990.
- [36] David Perry and Wolfgang Stadje. Duality of dams via mountain processes. *Operations Research Letters*, 31(6):451–458, 2003.
- [37] Narahari Umanath Prabhu. *Stochastic storage processes: queues, insurance risk, dams, and data communication*, volume 15. Springer Science & Business Media, 2012.
- [38] John Rice. On generalized shot noise. *Advances in Applied Probability*, 9(3):553–565, 1977.
- [39] Marian-Andrei Rizoïu, Swapnil Mishra, Quyu Kong, Mark Carman, and Lexing Xie. SIR-Hawkes: Linking epidemic models and Hawkes processes to model diffusions in finite populations. In *Proceedings of the 2018 World Wide Web Conference on World Wide Web*, pages 419–428. International World Wide Web Conferences Steering Committee, 2018.
- [40] Michael Rubinovitch and JW Cohen. Level crossings and stationary distributions for general dams. *Journal of Applied Probability*, 17(1):218–226, 1980.
- [41] Walter Rudin. *Principles of mathematical analysis*, volume 3. McGraw-hill New York, 1964.
- [42] Paul Sawers. Ottopias remote assistance platform for autonomous cars combines humans with ai. *VentureBeat*, 2018. URL <https://venturebeat.com/2018/12/21/ottopias-remote-assistance-platform-for-autonomous-cars-combines-humans-with-ai/>. Accessed: 6/21/2019.

- [43] J Sullivan, L Crone, and J Jalickee. Approximation of the unit step function by a linear combination of exponential functions. *Journal of Approximation Theory*, 28(4):299–308, 1980.
- [44] Sebastian Thrun. Efficient exploration in reinforcement learning. *Technical Report. Carnegie Mellon University*, 1992.
- [45] Waymo LLC. Autonomous vehicle disengagement reports. *California Department of Motor Vehicles*, 2018. URL [https://www.dmv.ca.gov/portal/dmv/detail/vr/autonomous/disengagement\\_report\\_2018](https://www.dmv.ca.gov/portal/dmv/detail/vr/autonomous/disengagement_report_2018).
- [46] Ronald W Wolff. Poisson arrivals see time averages. *Operations Research*, 30(2): 223–231, 1982.
- [47] Geoffrey Yeo. A dam with general release rule. *The ANZIAM Journal*, 19(4): 469–477, 1976.
- [48] GF Yeo. A finite dam with exponential release. *Journal of Applied Probability*, 11 (1):122–133, 1974.